Ground Motions in the Central United States

Gail M. Atkinson

Dept. Earth Sciences

Carleton University

Carleton UNIVERSITY

Canada's Capital University

POLARIS

Ground motion relations

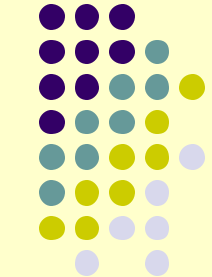

- Knowledge of ground motions is expressed as relations giving parameters such as peak ground acceleration (PGA) and response spectra as functions of magnitude and distance
- Ground motion relations are a key input to seismic hazard analysis
- Uncertainty in ground motion relations is typically the largest source of uncertainty in estimation of seismic hazard

What is known about ground motions in the CUS (Midcontinent)

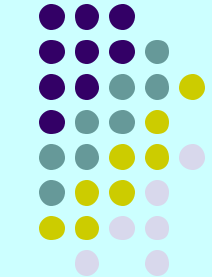

- Ground motion models (alternative relations)
- Ground motion data
- Issues in earthquake source
- Issues in earthquake path
- Overview of uncertainties in ground motion relations

CUS (Midcontinent) Ground Motion Relations: Models

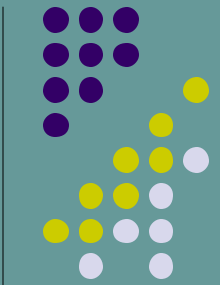

- Studies (EPRI, 1993) have shown that attenuation should be similar throughout the Midcontinent region (Central U.S., eastern U.S., southeastern Canada) – therefore I address entire midcontinent as a whole
- There are insufficient ground-motion data in the magnitude-distance range of engineering interest to directly obtain ground-motion relations by regression analysis
- Thus CUS relations are developed from models, which may be validated with data to varying degrees

Types of models used in development of ENA ground motion relations

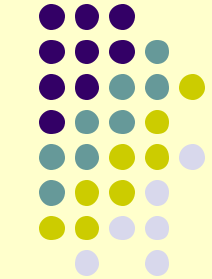

- Stochastic point source (single corner source) eg. Toro et al., 1997; Frankel et al., 1996
- Stochastic point source (double corner source) eg. Atkinson and Boore, 1995
- Hybrid empirical model (eg. Campbell, 2003)
- Finite-source/Green function numerical (eg. Somerville et al., 2001)
- Stochastic finite fault (eg. Atkinson and Boore, 2005)

Example of alternative ENA ground motion relations (EPRI, 2004)

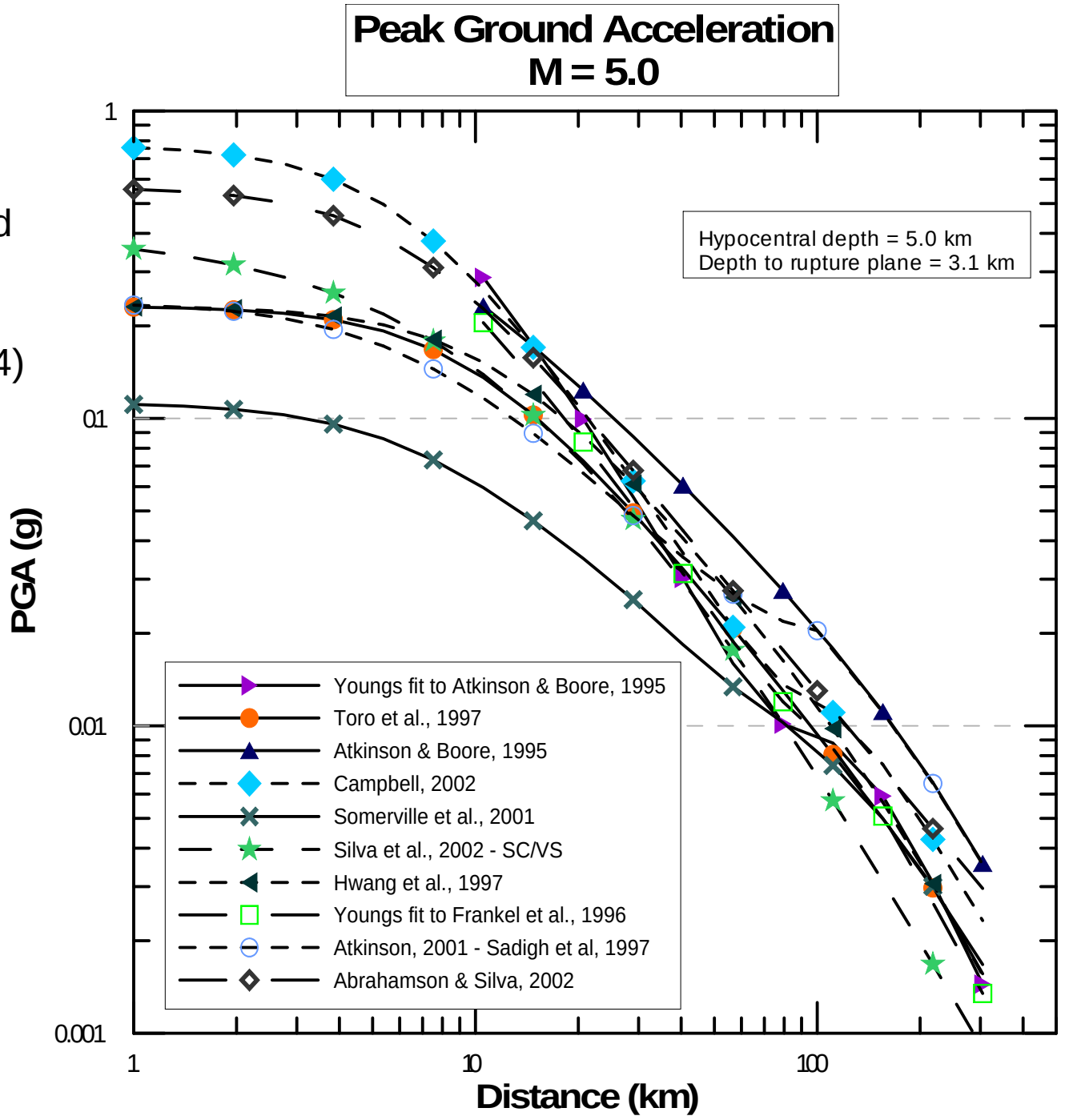

Example of alternative ENA ground motion relations (EPRI, 2004)

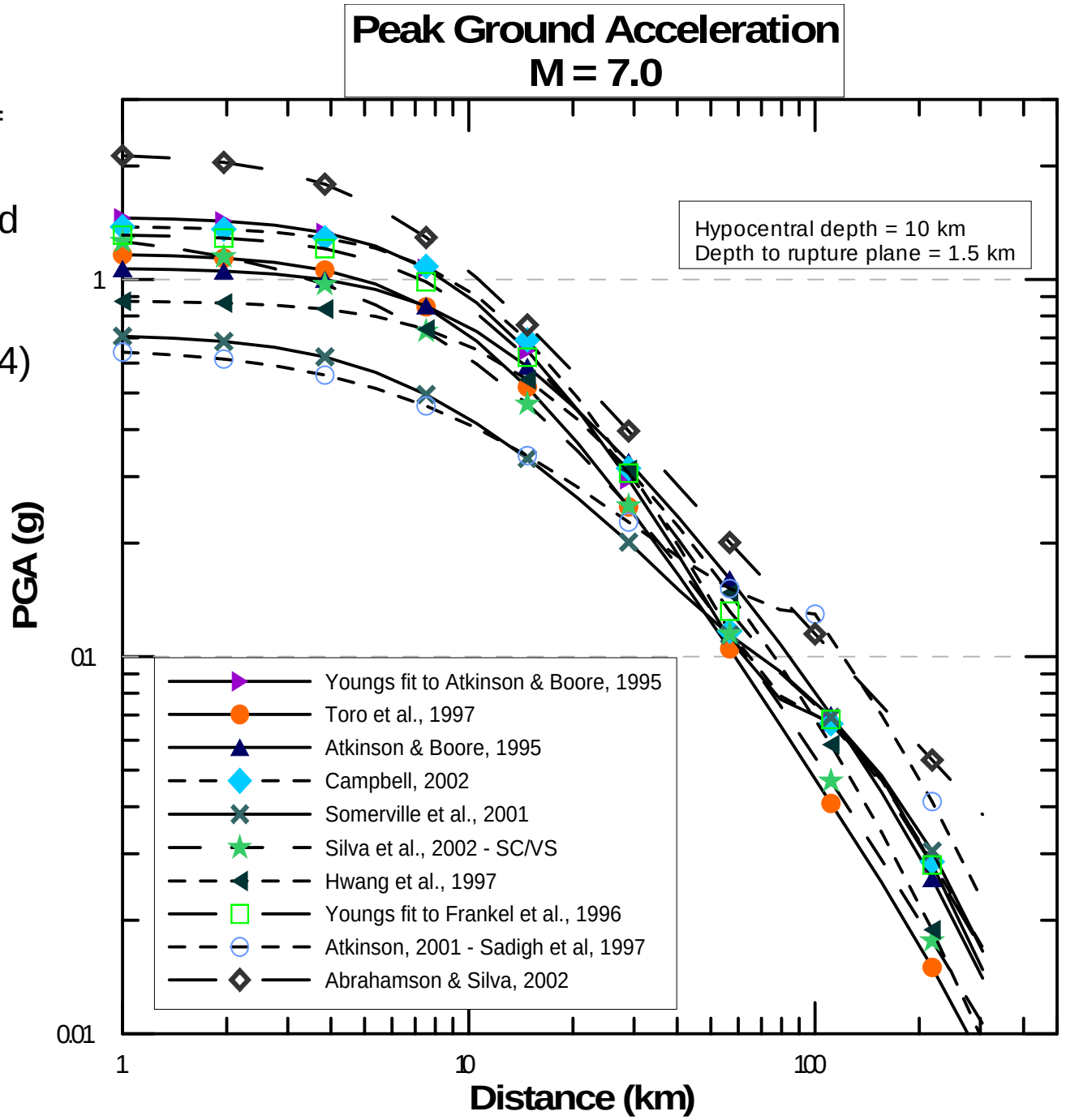

Example of alternative ENA ground motion relations (EPRI, 2004)

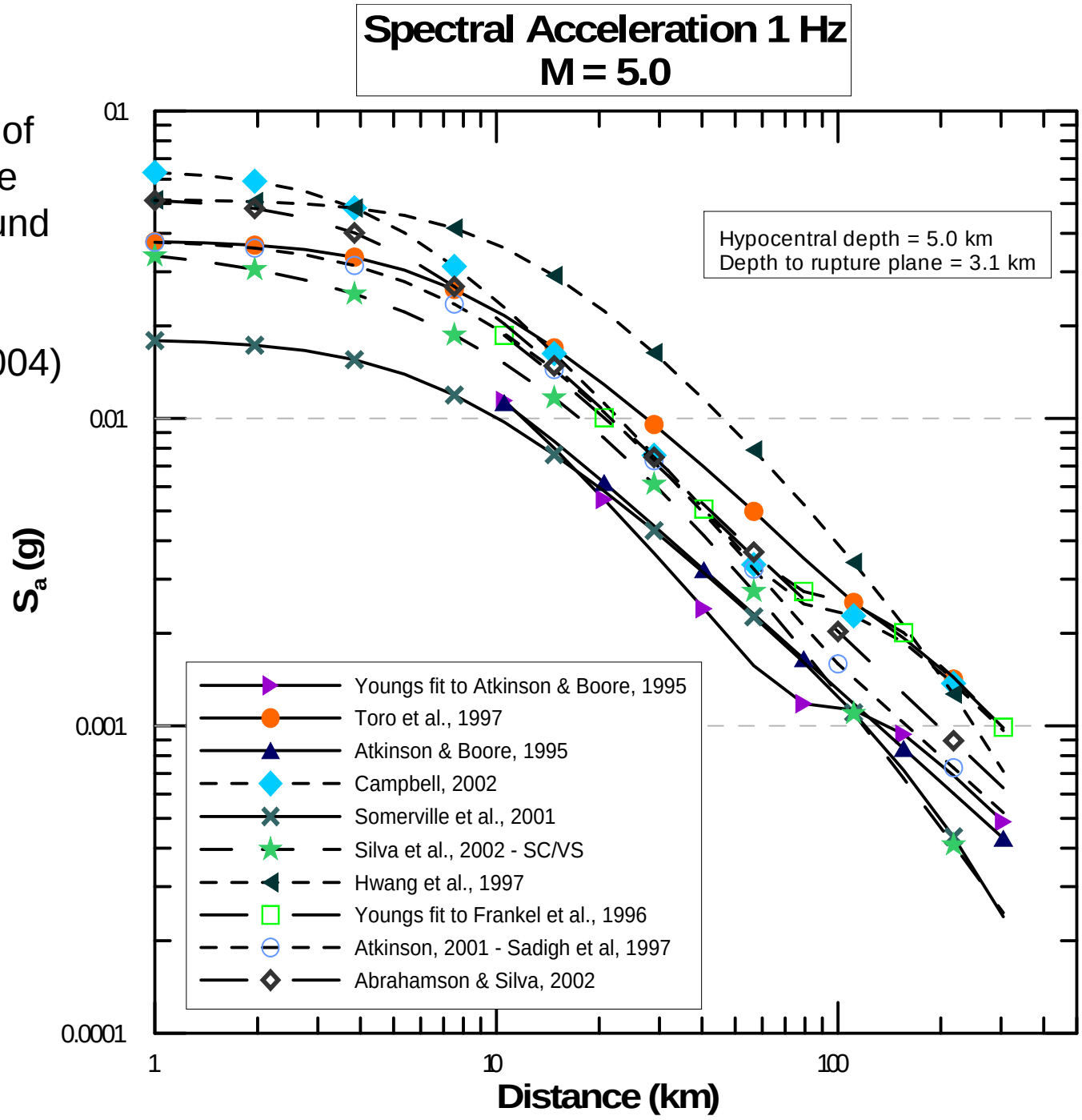

Example of alternative ENA ground motion relations (EPRI, 2004)

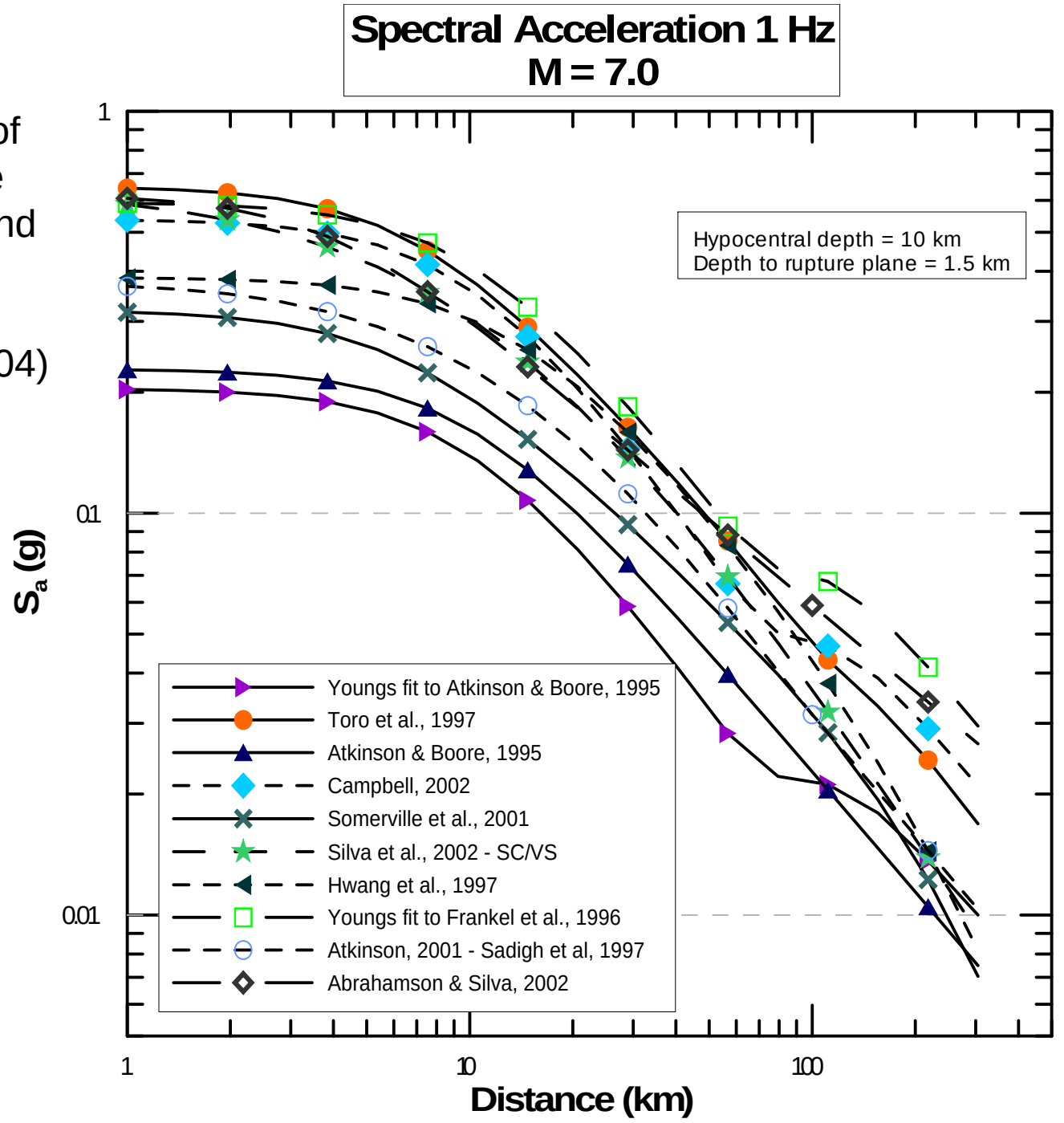

Example of alternative ENA ground motion relations (EPRI, 2004)

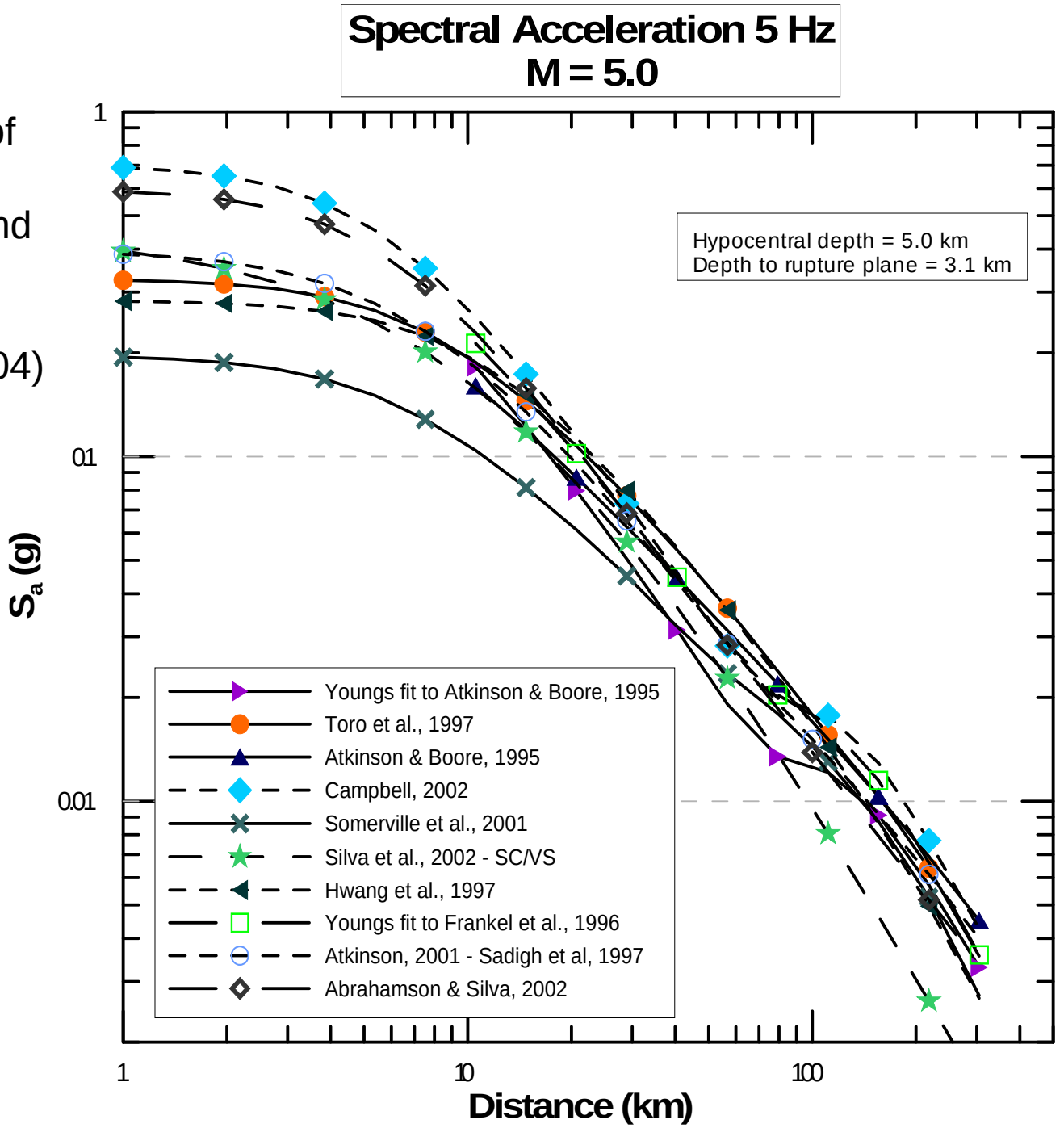

Example of alternative ENA ground motion relations (EPRI, 2004)

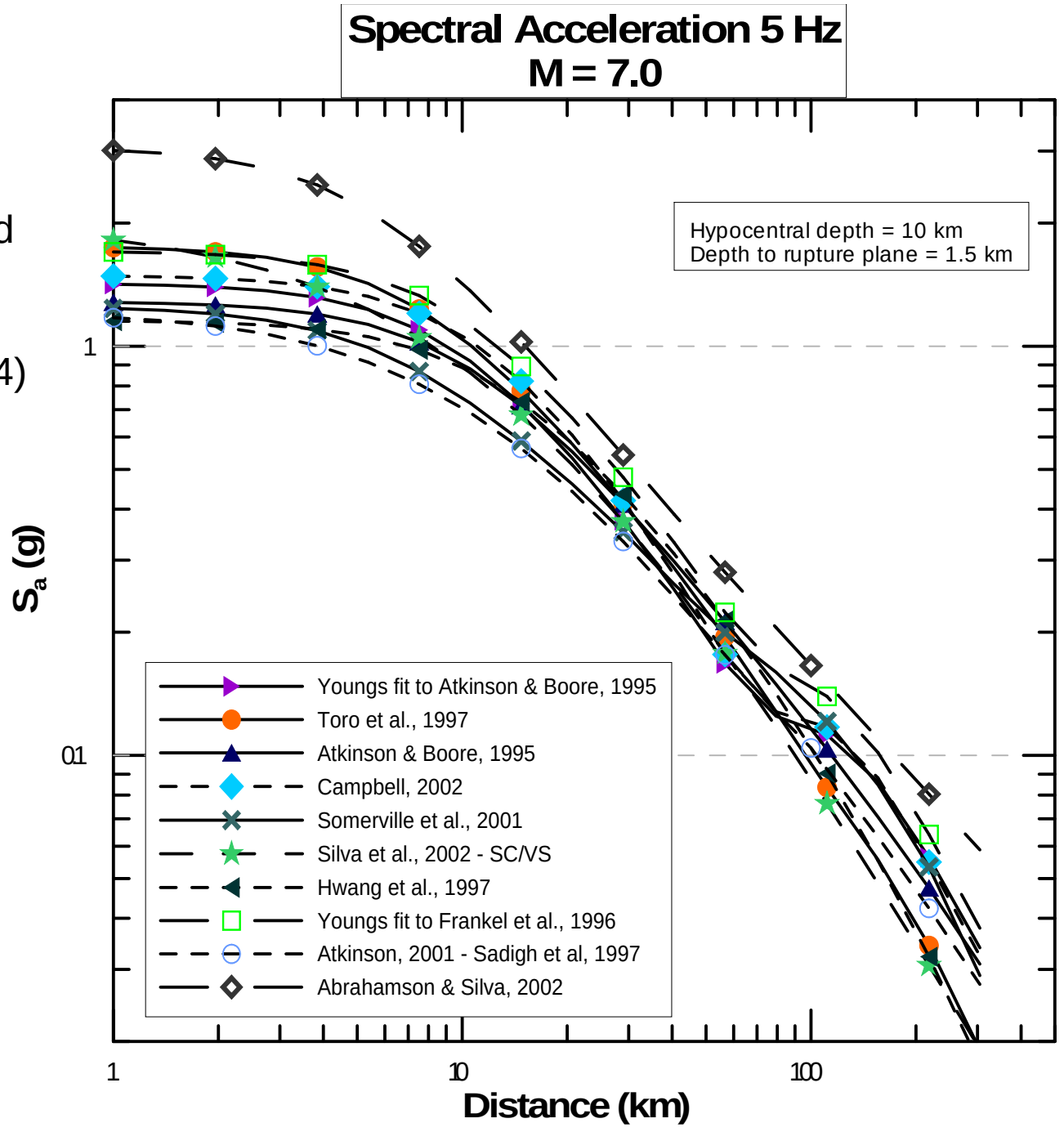

Overview of relations

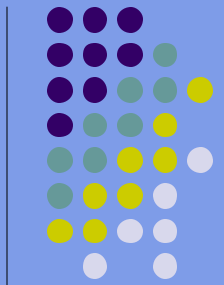

- EPRI (2004) provided overall synthesis and evaluation of the four main types of ground motion relations (to 2003)
- Results given as family of alternative relations expressing overall epistemic uncertainty (ie. uncertainty in modeling)
- Model for aleatory uncertainty (random variability) also provided

Note that in hazard analysis both epistemic and aleatory uncertainty in ground motion relations are important input parameters.

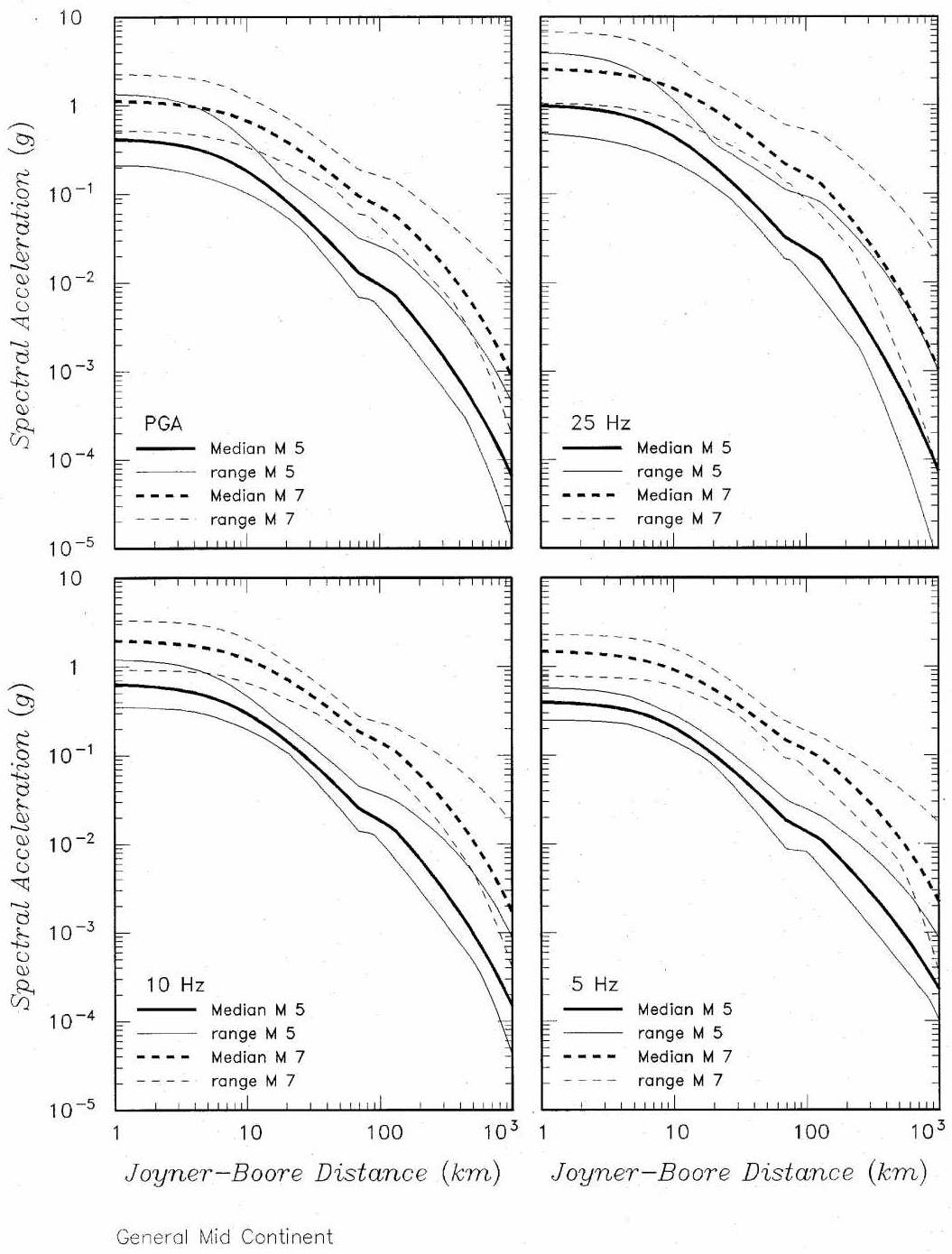

General Mid Continent

Range of models for M5 and M7 (EPRI, 2004)

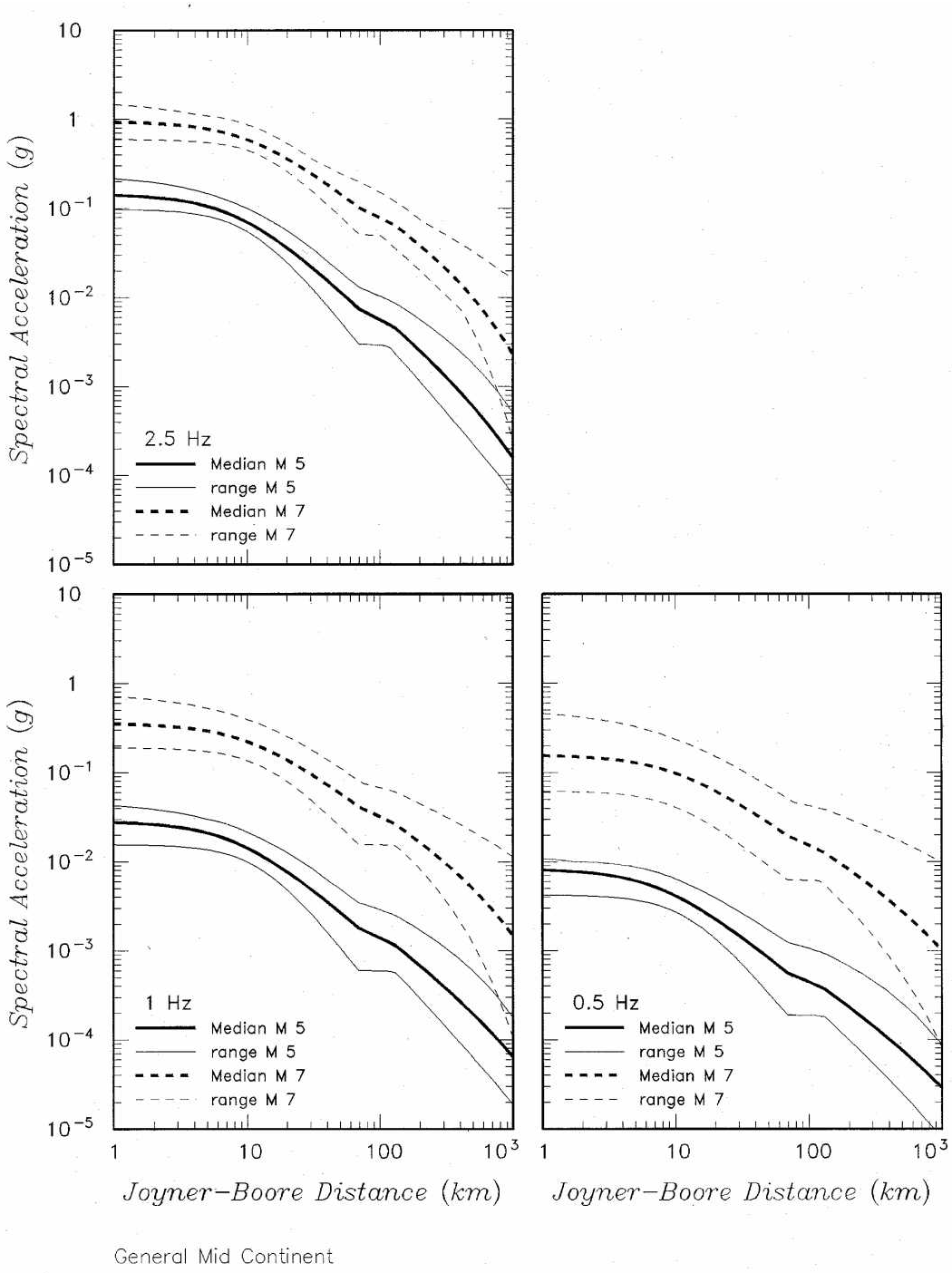

General Mid Continent

Range of models for M5 and M7 (EPRI, 2004)

Ground Motion Data (ENA)

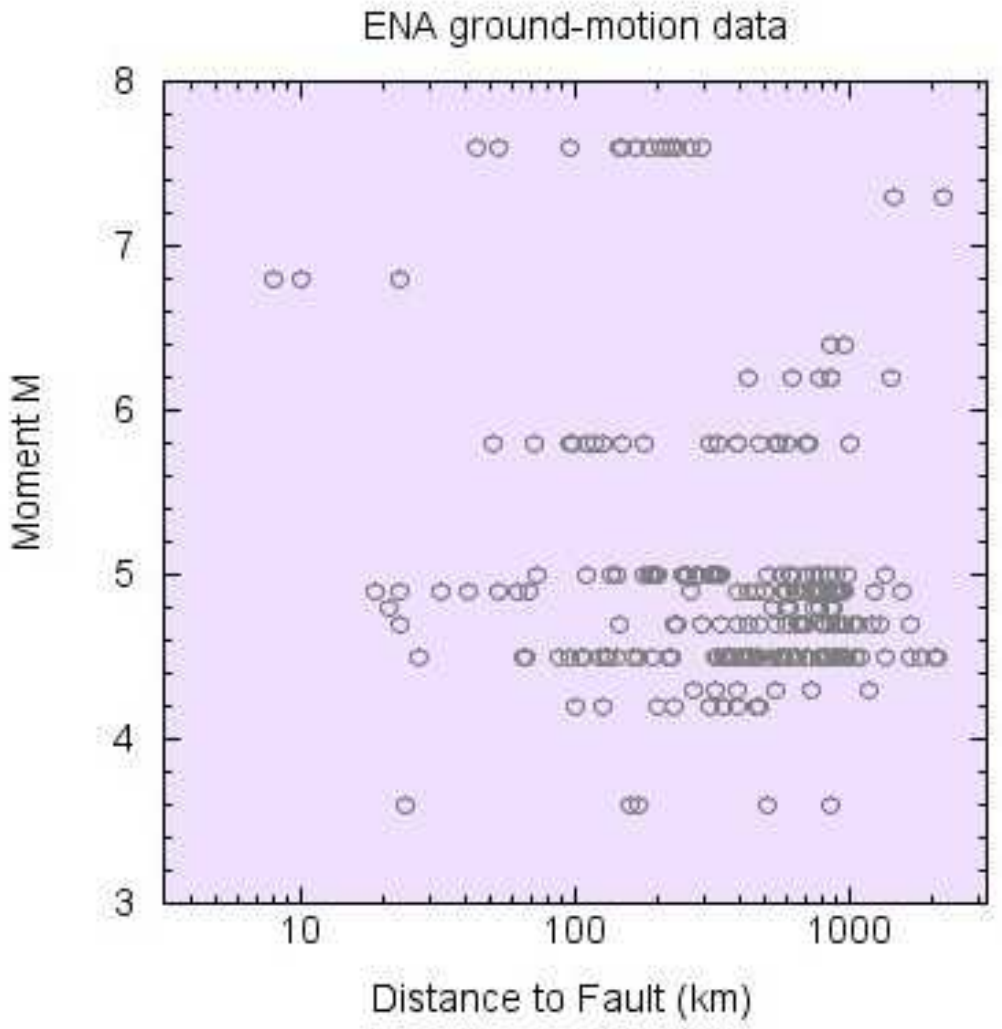

Atkinson and Boore 2005 relations

- Based on stochastic finite-fault model (of Motazedian and Atkinson, 2005)
- Key source parameter is stress drop – determined from compilation of instrumental and historical data
- Attenuation model based on empirical trilinear model of Atkinson, 2004 for ENA

Stochastic finite fault model (Silva; Beresnev and Atkinson; *Motazedian and Atkinson, 2005*)

STOCHASTIC FINITE-FAULT MODEL
(Beresnev and Atkinson, 1997, 1998)

TREAT FINITE FAULT PLANE AS AN ARRAY OF SUBFAULTS

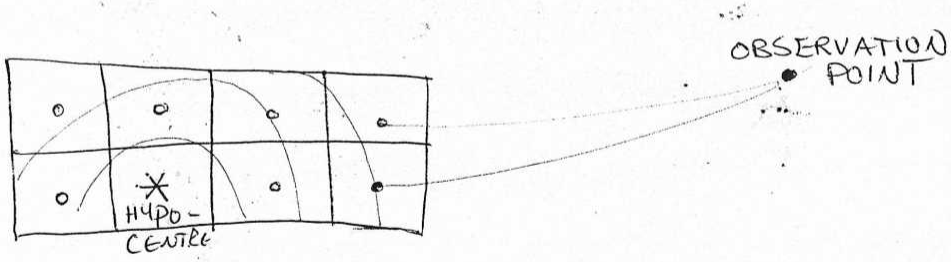

MODEL EACH SUBFAULT AS A STOCHASTIC POINT SOURCE, WITH A BRUNE (ω^2) SOURCE SPECTRUM

RUPTURE STARTS AT A SPECIFIED SUBFAULT (HYPOCENTRE), AND PROPAGATES IN ALL DIRECTIONS WITH SPECIFIED RUPTURE PROPAGATION VELOCITY (SAY 0.8 TIMES SHEAR WAVE VELOCITY).

SUBFAULT RADIATION IS 'TRIGGERED' WHEN RUPTURE REACHES THE CENTRE OF THE SUBFAULT

CONTRIBUTIONS TO RADIATION AT OBSERVATION POINT ARE SUMMED OVER ALL SUBFAULTS.

Parameters needed to apply stochastic finite-fault model

- All parameters needed for stochastic point source model
- Geometry of source (can assume fault plane based on empirical relations such as Wells and Coppersmith on fault length and width vs. M)
- Direction of rupture propagation (assumed random)
- Slip distribution on fault (assumed random)

Some features of Motazedian and Atkinson (2005) stochastic finite fault model:

• simulations independent of subfault size (conservation of radiated energy)
• model applicable over wide range of magnitudes (can simulate M 4 to 8 with single consistent model)
• incorporation of “self-healing” behavior

Self-healing model: in the lower panel, only part of the fault is slipping at any one time

Figure 3.a 100 % Pulsing area

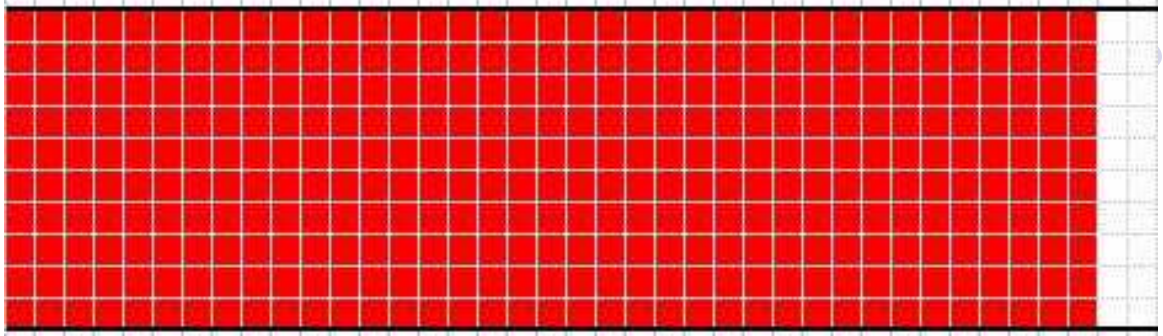

Figure 3.b 25% Pulsing area

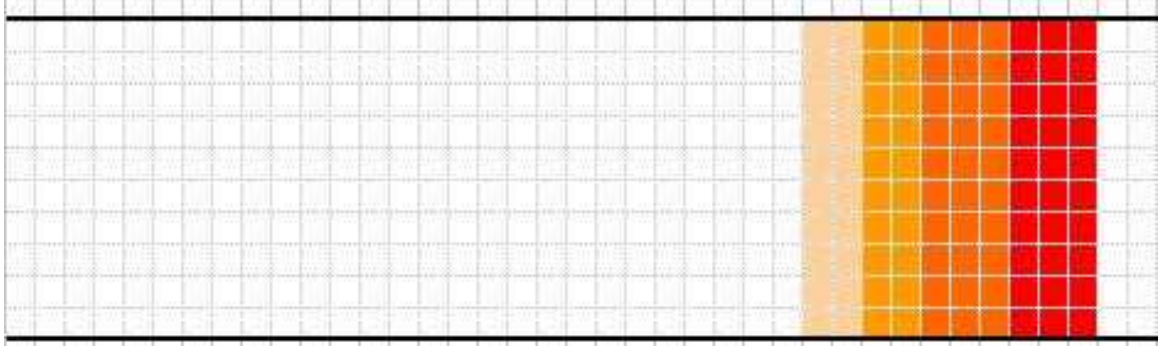

Figure 3.a-b. In the healing-front model (3.a) when a subfault ruptures, the total ruptured area contributes to the frequency content of the radiated wave from the rupturing subfault. In the self-healing model, a wave front has a tail which includes the pulsing subfaults and those subfaults that are still sliding. In the self-healing model (3.b), the passive area (white cells) should not have any effect on the frequency content of the distant subfault.

The low-frequency spectral shape (and sag at intermediate frequencies) is controlled by the %pulsing area

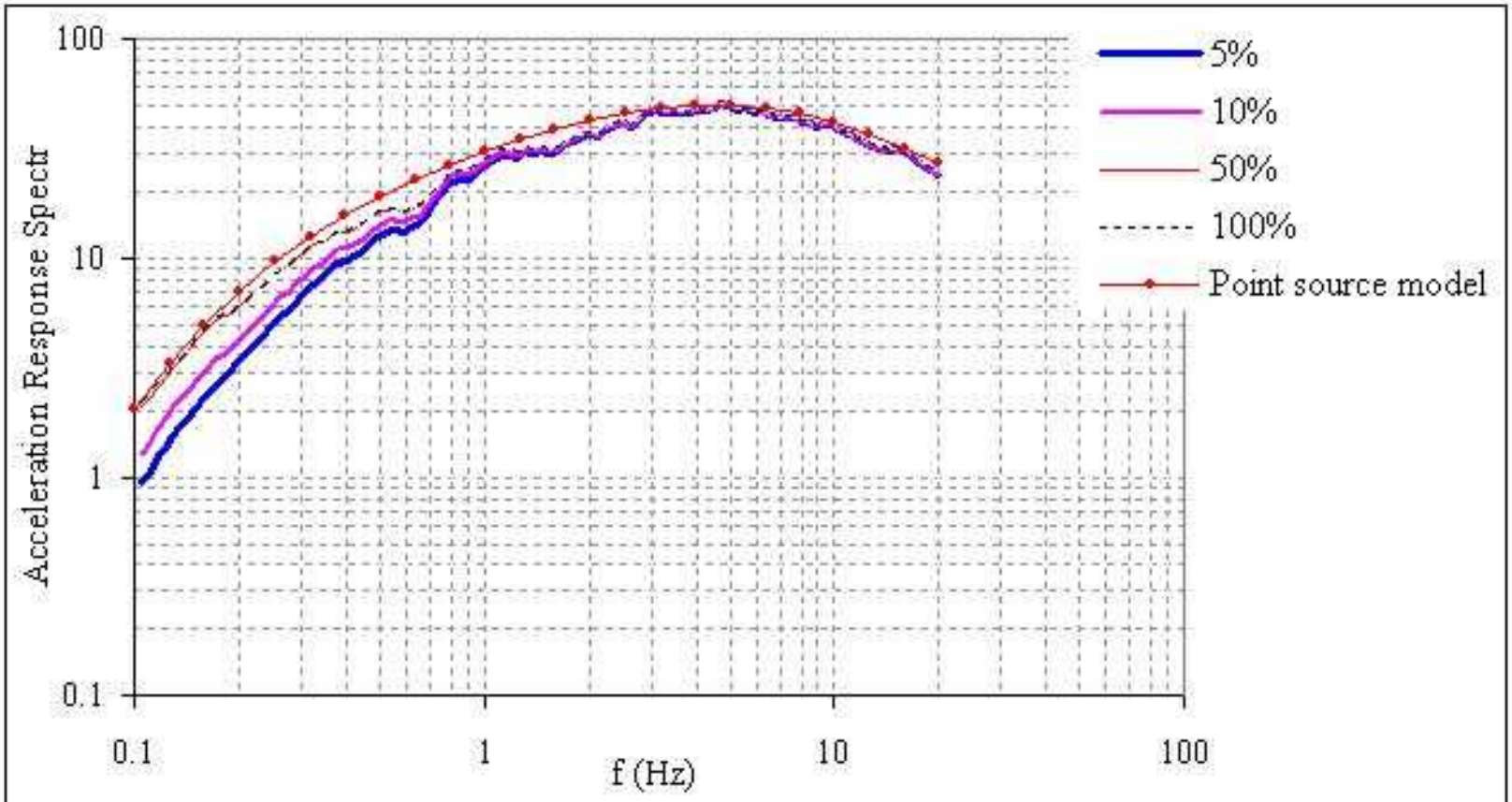

Fig 5. 5% damped pseudo-acceleration for event of M7.0 at R=100 km for different pulsing area percentages, using dynamic corner frequency and corresponding point-source model. In EXSIM, variation of pulsing area can be used to adjust the relative amplitudes of low-frequency motion in finite fault modeling. A narrow pulsing area results in lower amplitudes at longer periods.

Finite-fault model reproduces 2-corner shape of source spectrum that is observed empirically (thus providing an explanation as to why we obtain a 2-corner shape)

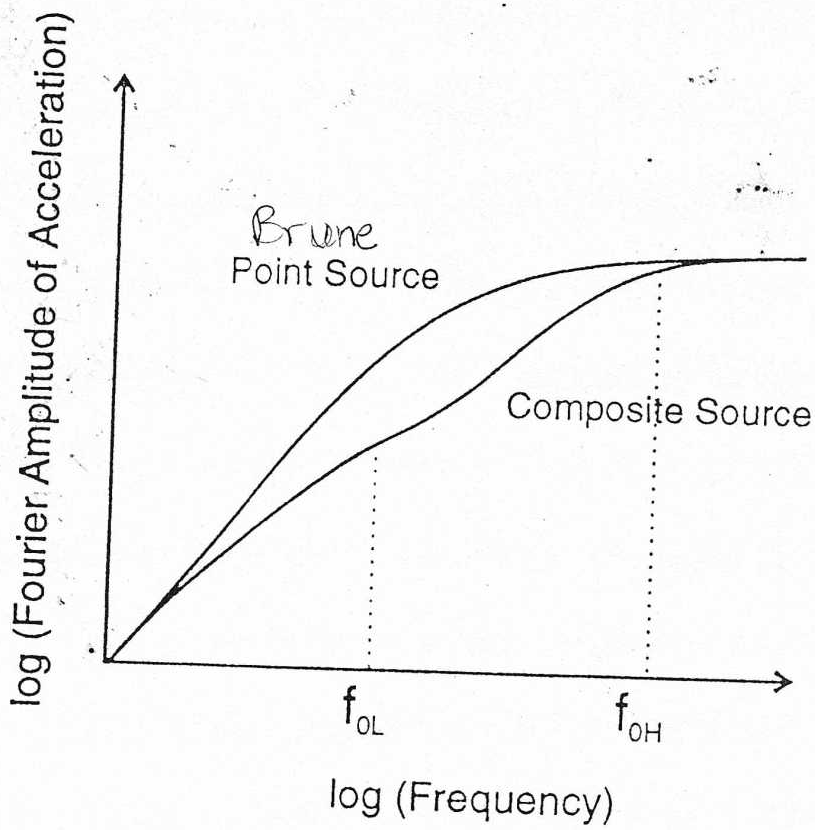

Figure 3. Comparison of the spectrum resulting from the summation of subevent point sources over a finite fault plane (lower line), with a single ω^2 spectrum, having the same moment magnitude and high-frequency spectral level (upper line). f_{0H} is the subfault corner frequency. f_{0L} is the second (low-frequency) corner produced by the summation procedure, under the conservation-of-moment constraint.

High-frequency spectral level depends on stress drop (as in point-source model)

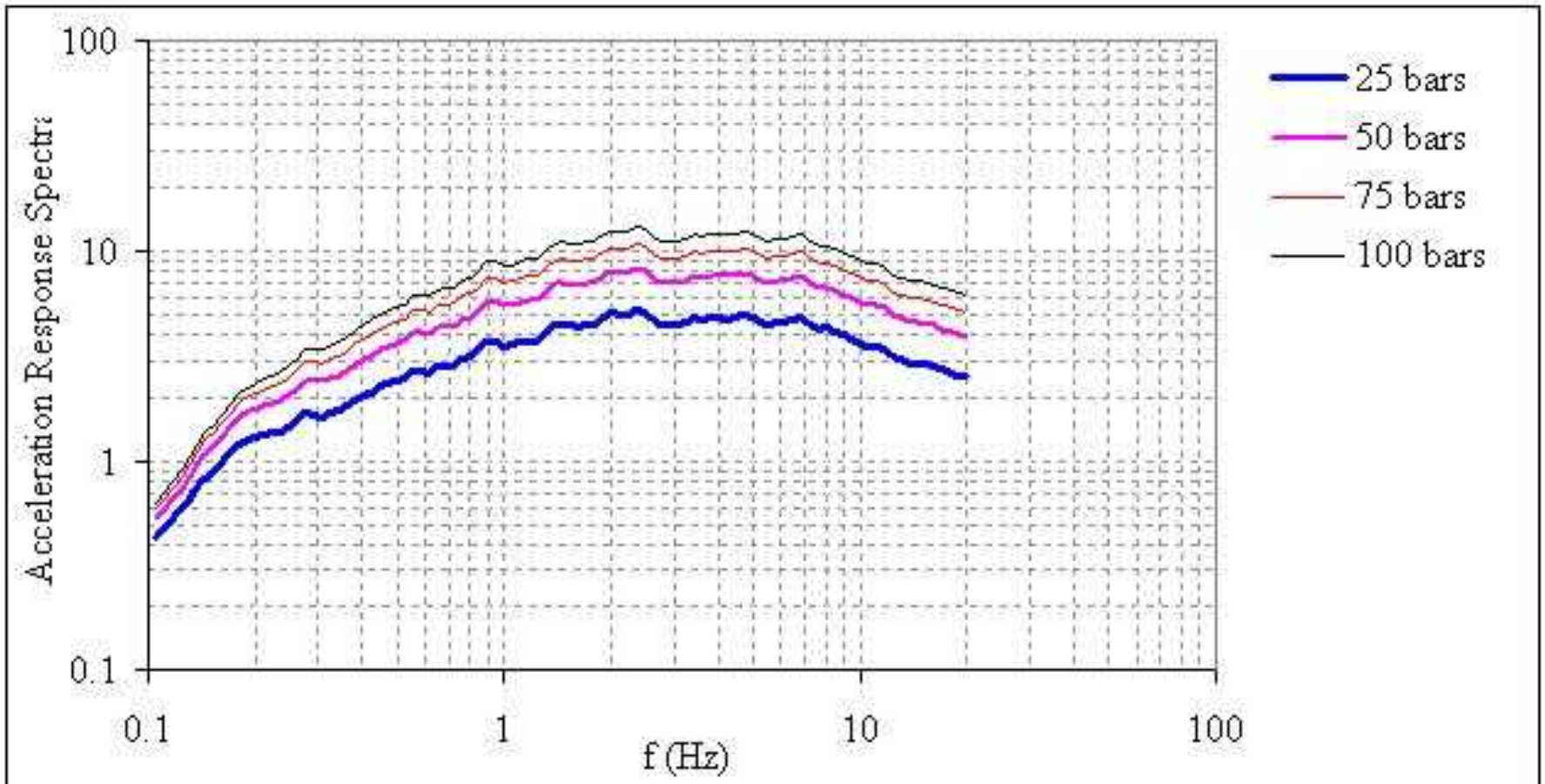

Fig 6. 5% damped pseudo-acceleration for event of M7.0 at R=333 km (25% pulsing area) for different stress parameter , using dynamic corner frequency. In EXSIM, variation of stress parameter can be used to adjust the relative amplitudes of high-frequency motion. By increasing the stress parameter, the amplitude of high frequencies increases.

Example Finite-fault stochastic simulation record

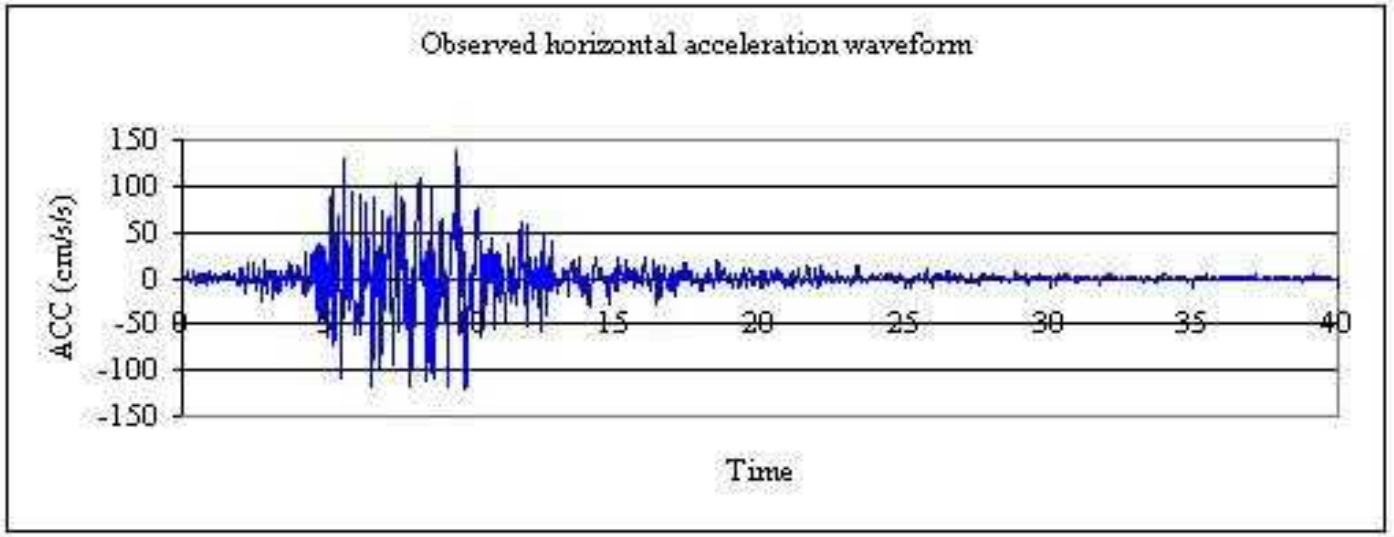

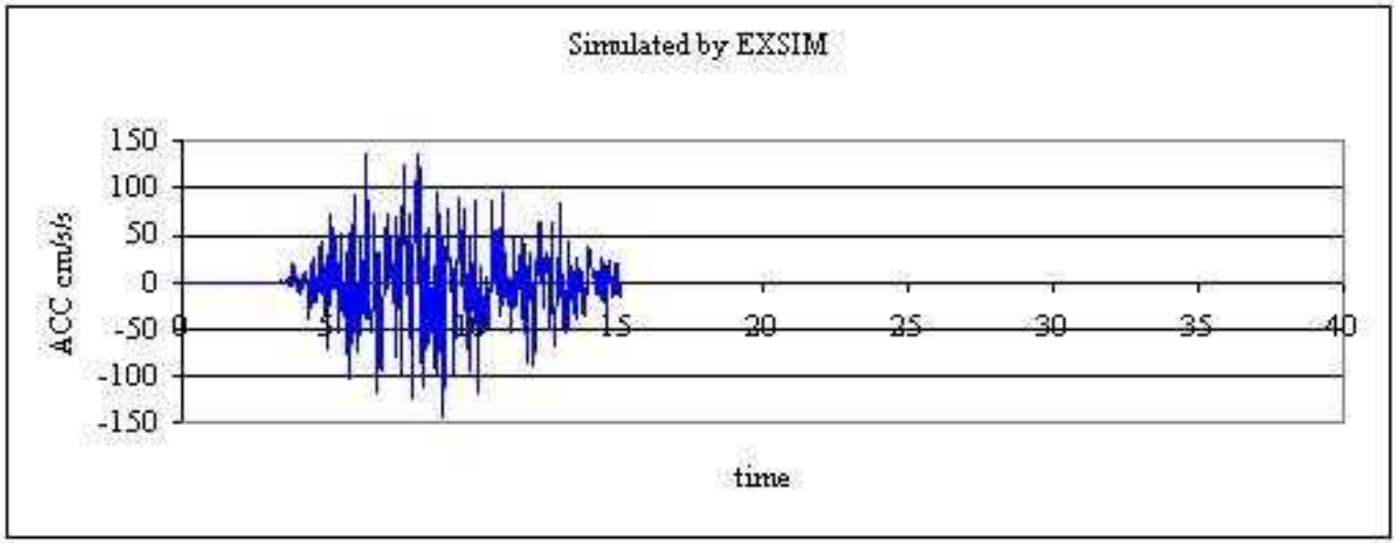

Figure 7. Simulated and observed horizontal acceleration waveform for M6.7, 1994 Northridge earthquake (Vasquez Rocks Park station).

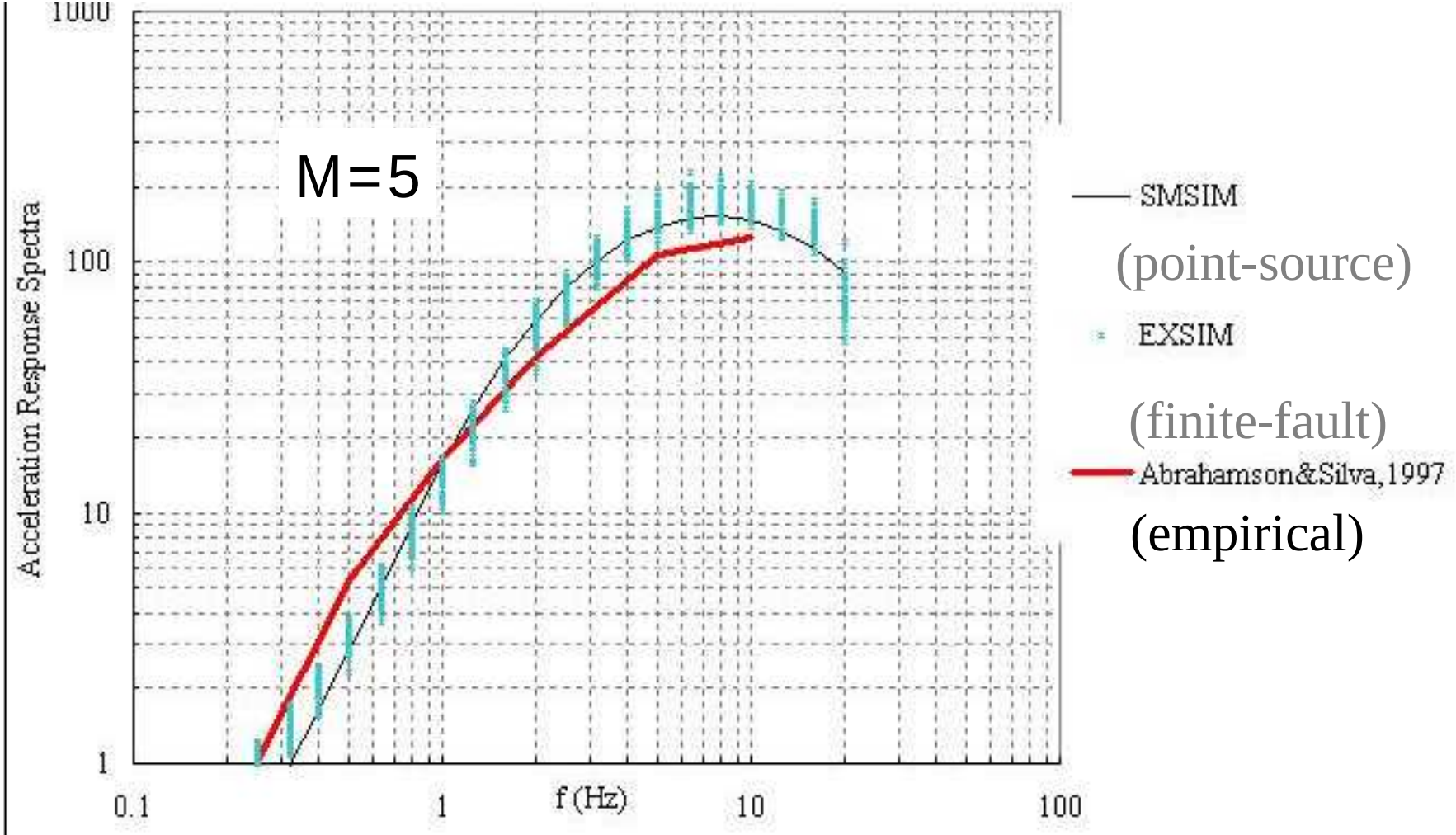

Fig 11. Comparison between response spectra from **M**5.0 point source modeling, SMSIM, Boore, 1995 (R=15 , stress drop=120 bars), Abrahamson and Silva ground motion relations for California, 1997 (R=15), and EXSIM(a profile of observation points around the fault plane with R=15 km and azimuth coverage from 0 to 180 degrees, stress drop=120 bars, and 50% pulsing area).

Comparison of finite fault, point source and empirical models for M5 in California

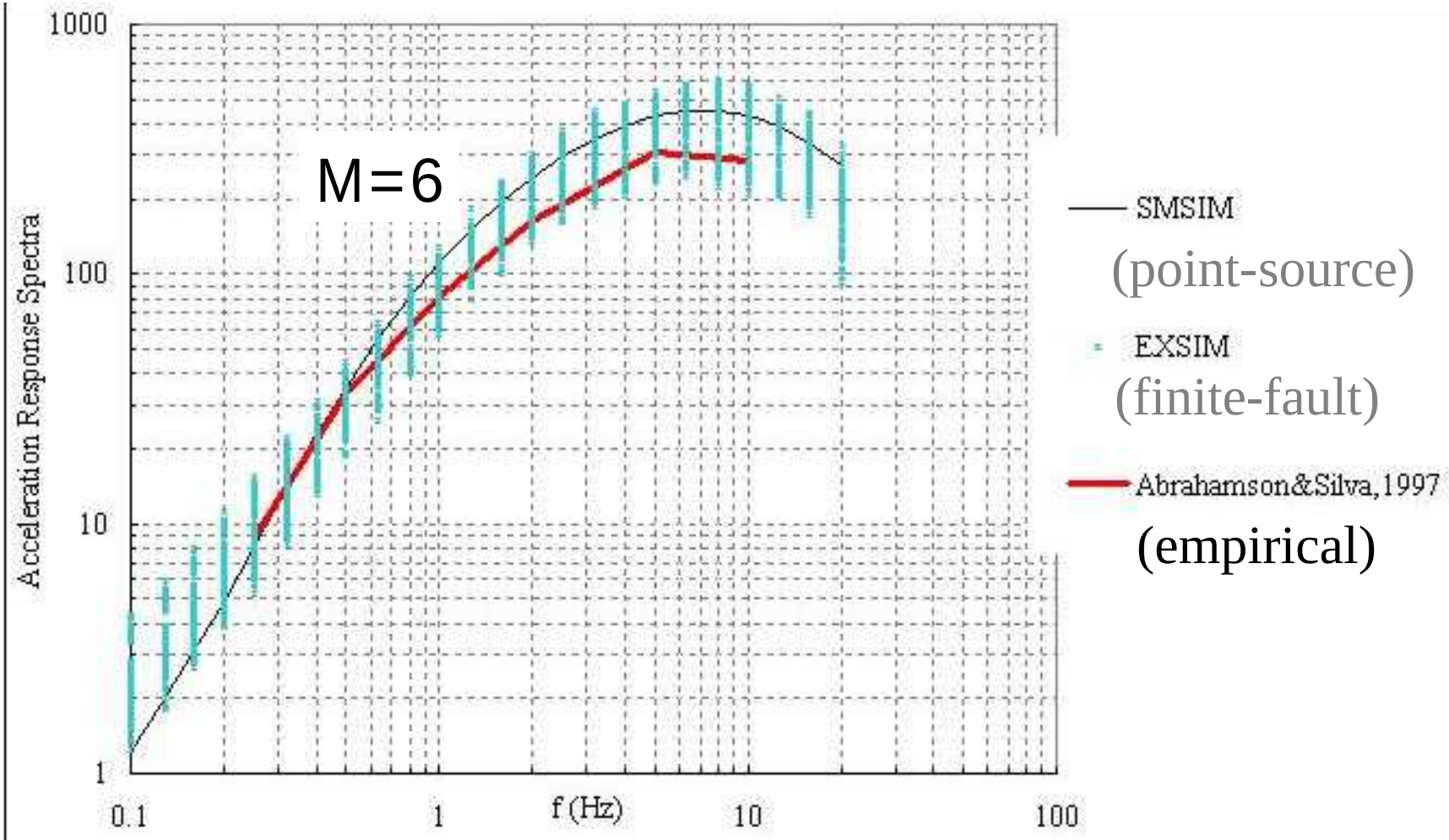

Fig 12. Comparison between response spectra from **M6**.0 point source modeling, SMSIM, Boore, 1995 (R=15 , stress drop=120 bars), Abrahamson and Silva ground motion relations for California, 1997 (R=15), and EXSIM(a profile of observation points around the fault plane with R=15 km and azimuth coverage from 0 to 180 degrees, stress drop=120 bars, and 50% pulsing area).

Comparison of finite fault, point source and empirical models for M6 in California

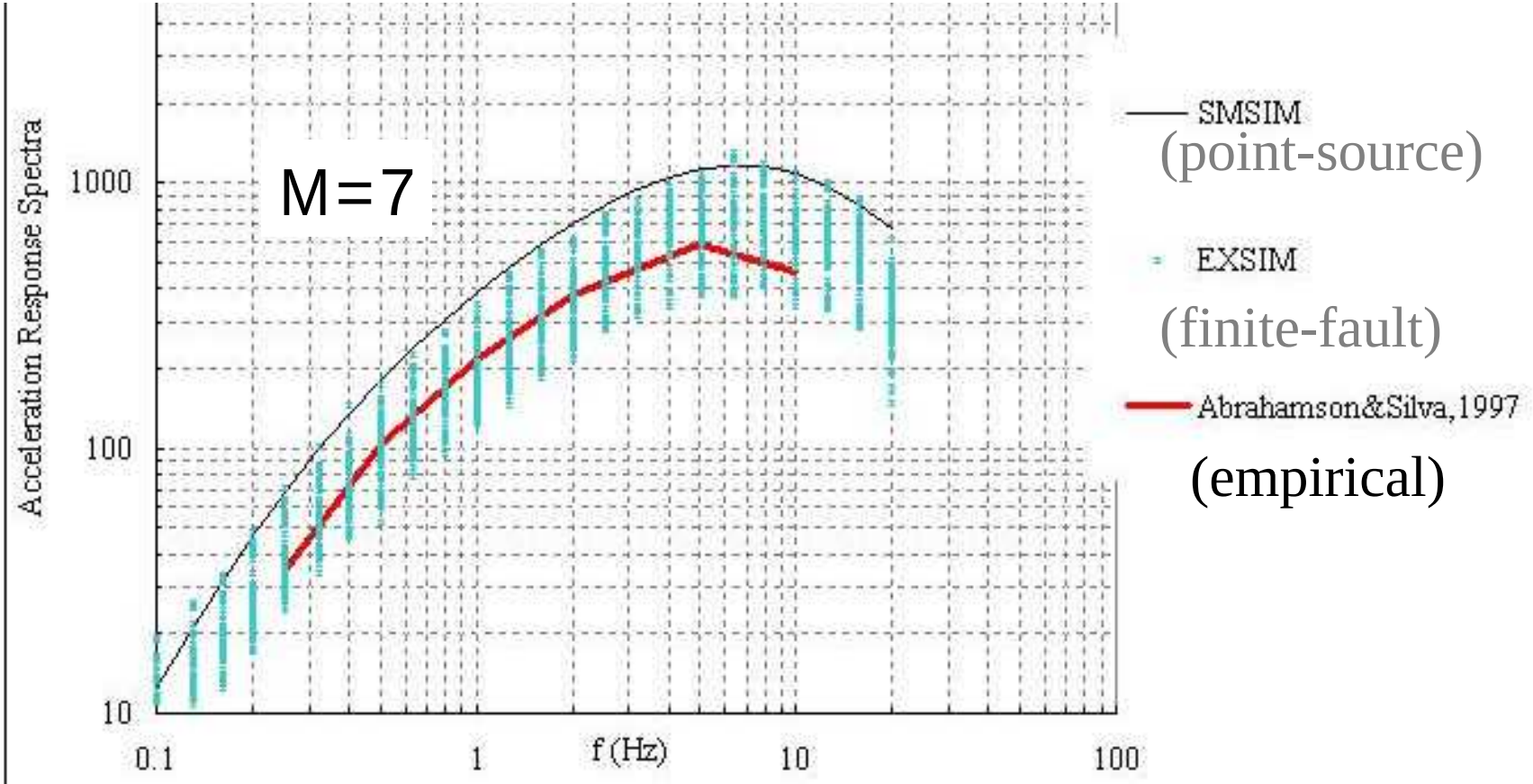

Fig 13. Comparison between response spectra from **M**7.0 point source modeling, SMSIM, Boore, 1995 (R=15 , stress drop=120 bars), Abrahamson and Silva ground motion relations for California, 1997 (R=15), and EXSIM(a profile of observation points around the fault plane with R=15 km and azimuth coverage from 0 to 180 degrees, stress drop=120 bars, and 50% pulsing area). Finite-fault effects in ground motions become important for larger earthquakes. Point source models of earthquake ground motion are inappropriate for earthquakes that rupture an extended fault plane.

Comparison of finite fault, point source and empirical models for M7 in California

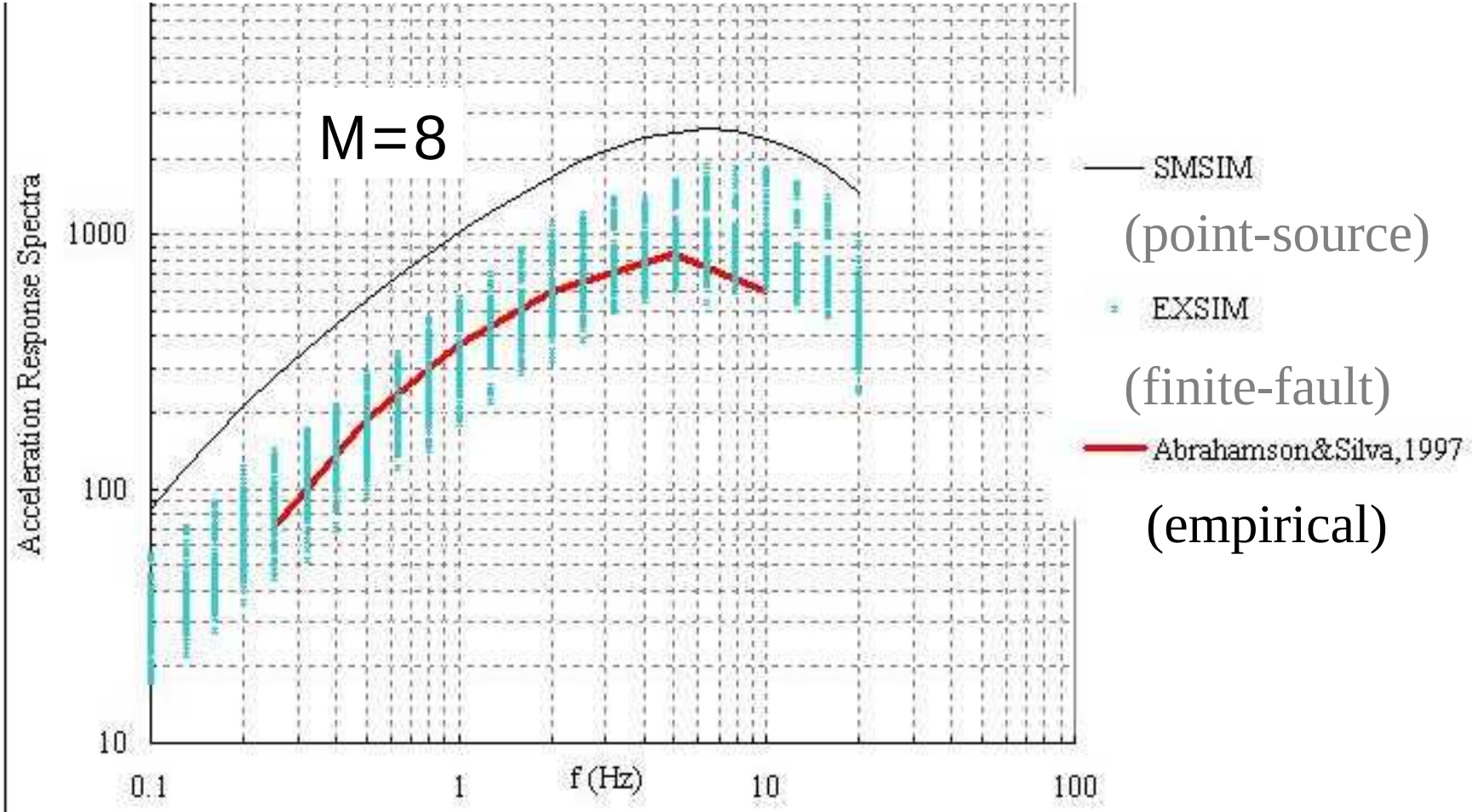

Fig 14. Comparison between response spectra from **M8**.0 point source modeling, SMSIM, Boore, 1995 (R=15 , stress drop=120 bars), Abrahamson and Silva ground motion relations for California, 1997 (R=15), and EXSIM(a profile of observation points around the fault plane with R=15 km and azimuth coverage from 0 to 180 degrees, stress drop=120 bars, and 50% pulsing area). Finite-fault effects in ground motions become important for larger earthquakes. Point source models of earthquake ground motion are inappropriate for earthquakes that rupture an extended fault plane.

Comparison of finite fault, point source and empirical models for M8 in California

ENA Model Parameters and their aleatory variability (AB05)

Parameter	Distribution type	Median	Standard Deviation	Minimum	Maximum
Fault Dip	Normal	50.	20.	10.	90.
Log stress	Normal	2.14	0.31		
Pulsing%	Random			10.	90.
Kappa	Random			0.002	0.01
b1 (R<70)	Random	-1.3		-1.5	-1.1
b2 (70-140)	Random	+0.2		-0.5	+0.9
Depth	Normal	13.	10.	2.	30.
Fault length factor	Random			0.2	0.8
Fault width factor	Random			0.4	1.0

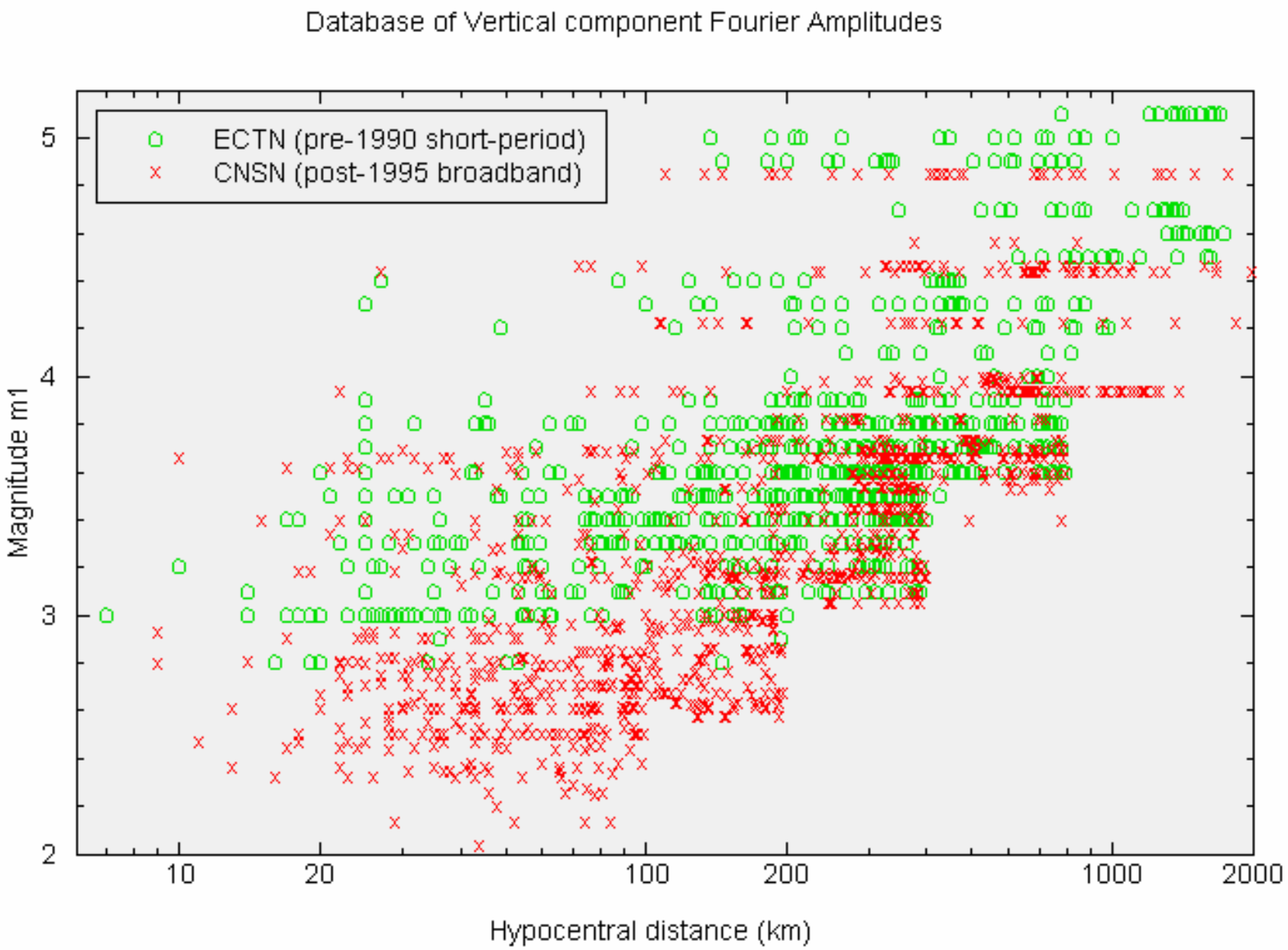
Database of Vertical component Fourier Amplitudes
ECTN (pre-1990 short-period)
CNSN (post-1995 broadband)
Magnitude m1
5
4
3
2
10
20
100
200
1000
2000
Hypocentral distance (km)

Illustration of typical decay of spectral amplitudes for m1=3.75. Line is trilinear shape fitted to the data. Transition distances are r01=70 km, ro2 = 140 km. Slopes of geometric attenuation: -1.3, +0.2, -0.5

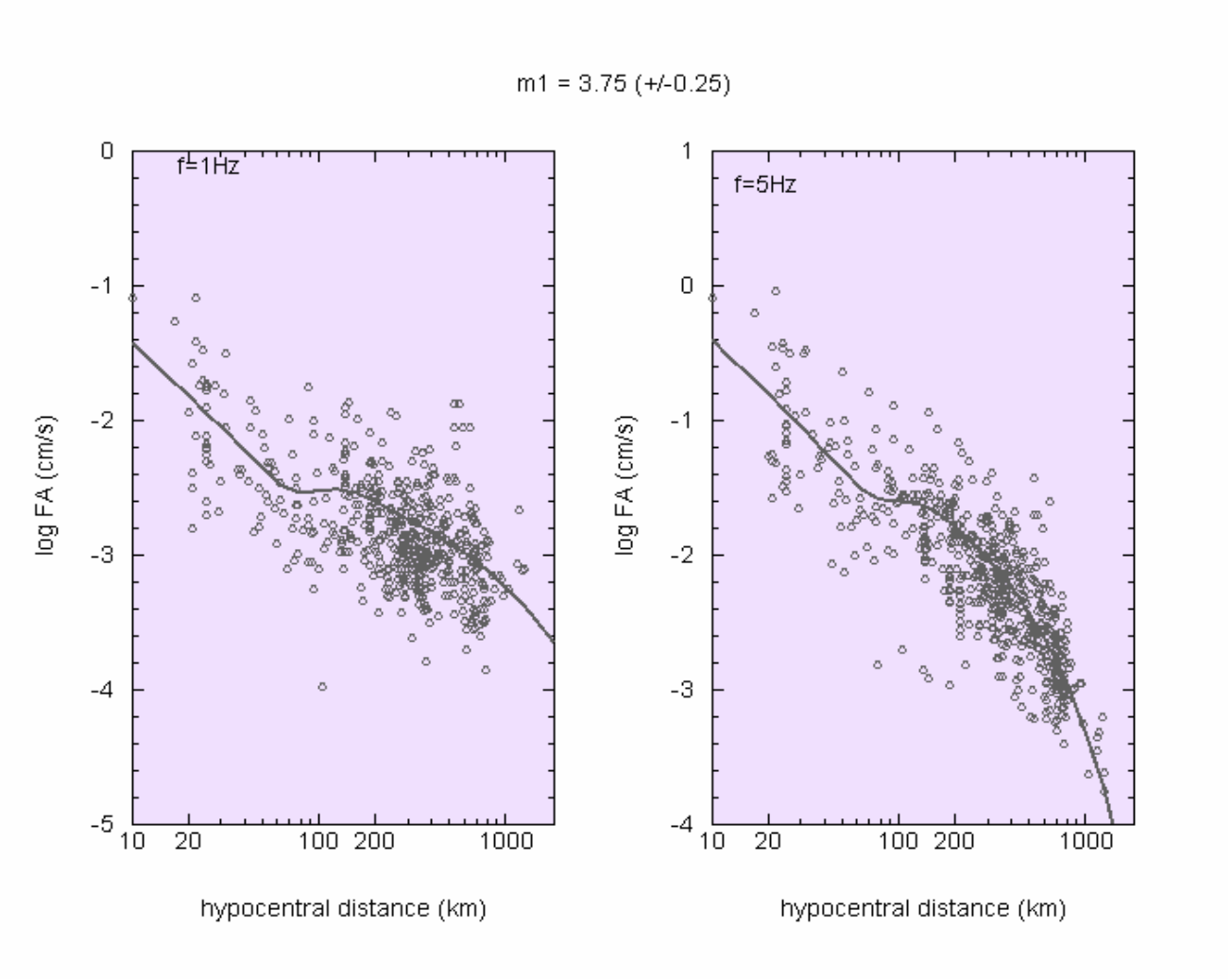

Amplitudes decay faster than 1/R at R<70 km. This has important implications for ENA ground motion relations.

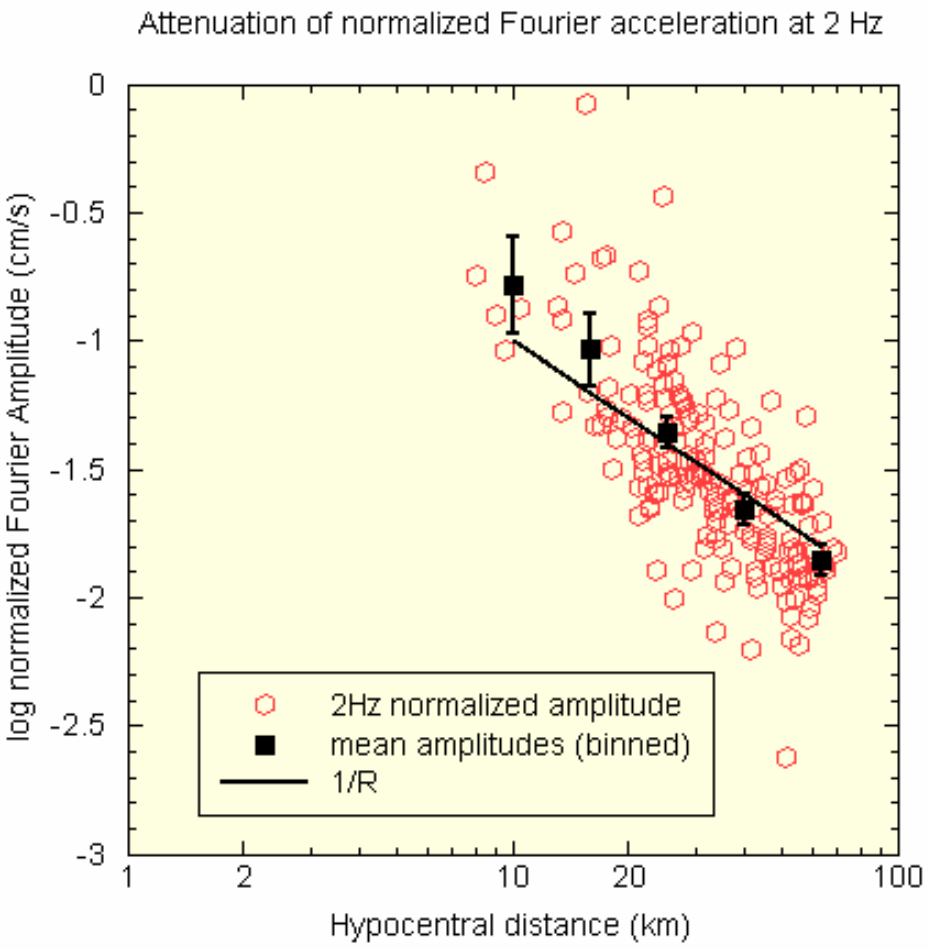

Residuals versus distance (1 and 5 Hz) for regression model (attenuation transitions r01, r02, geometric spreading slopes -1.3, +0.2, -0.5)

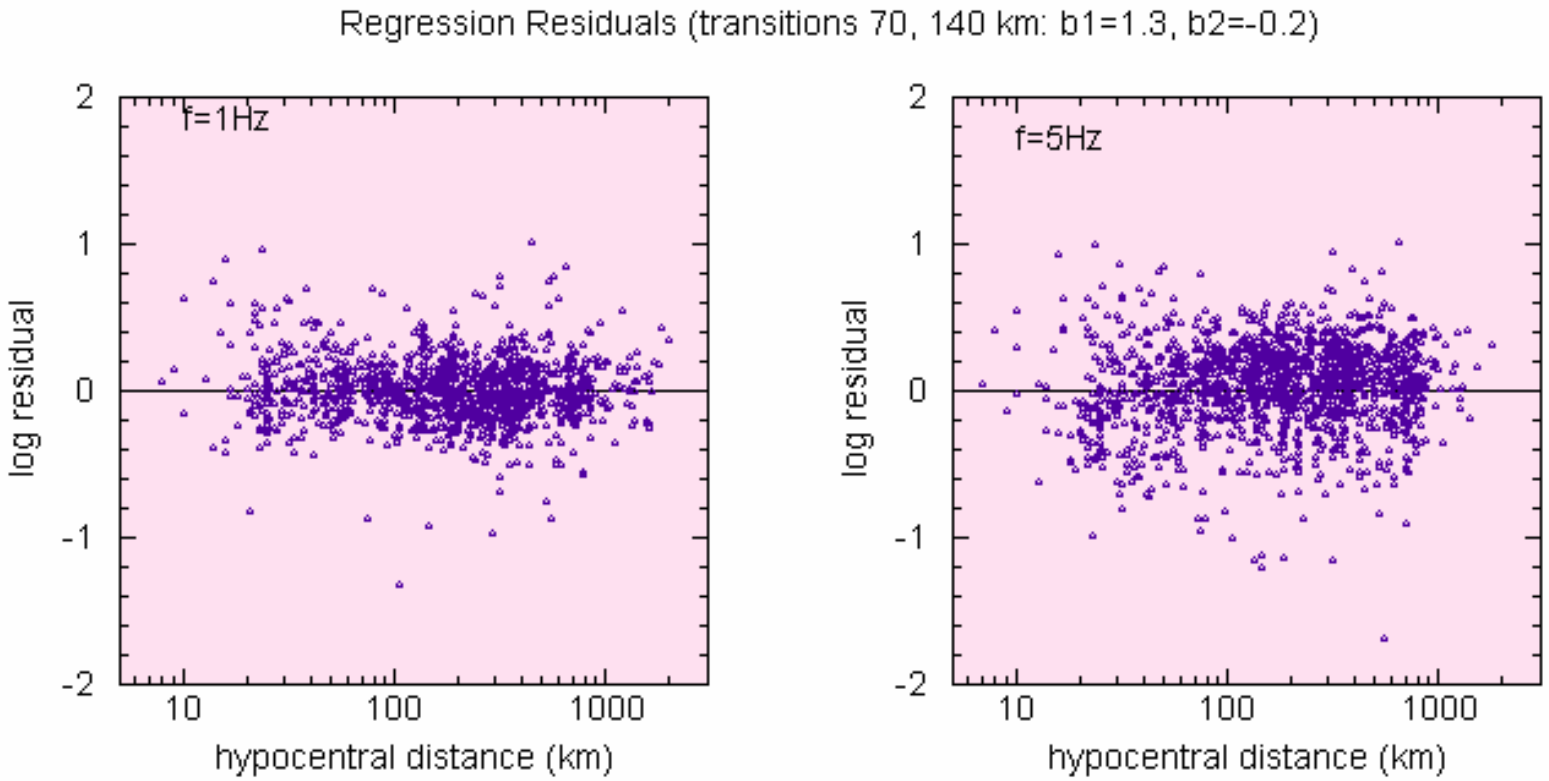

Regression residuals show distance trends when broken down by focal depth: deeper events attenuate more slowly than shallow events, especially at high frequencies

A correction factor to the attenuation based on focal depth was developed to account for the depth-dependence of attenuation:

Log Correction Factor

= d1 (h-10) log R +d2

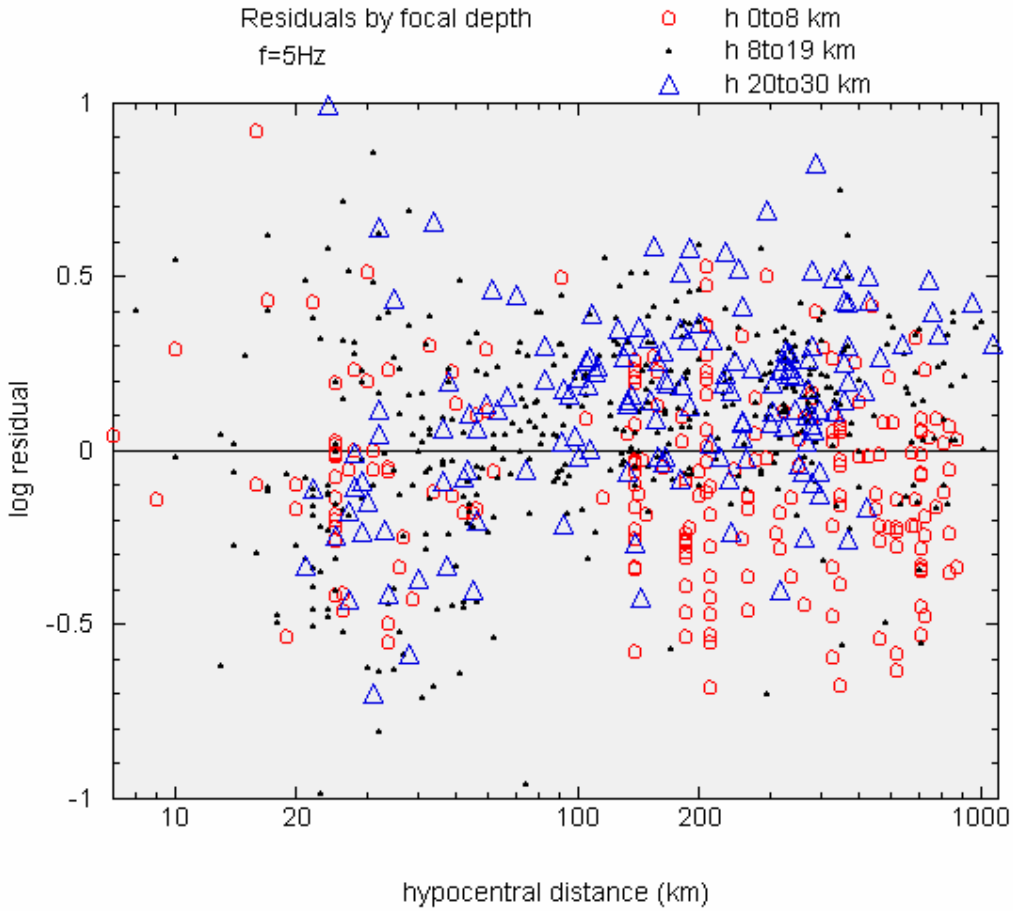

Evaluate whether the horizontal component attenuates differently than the vertical: apply the regression equation developed for the vertical component to the horizontal component data, and examine residuals (log observed – log predicted) versus distance.

Mean residual = H/V.

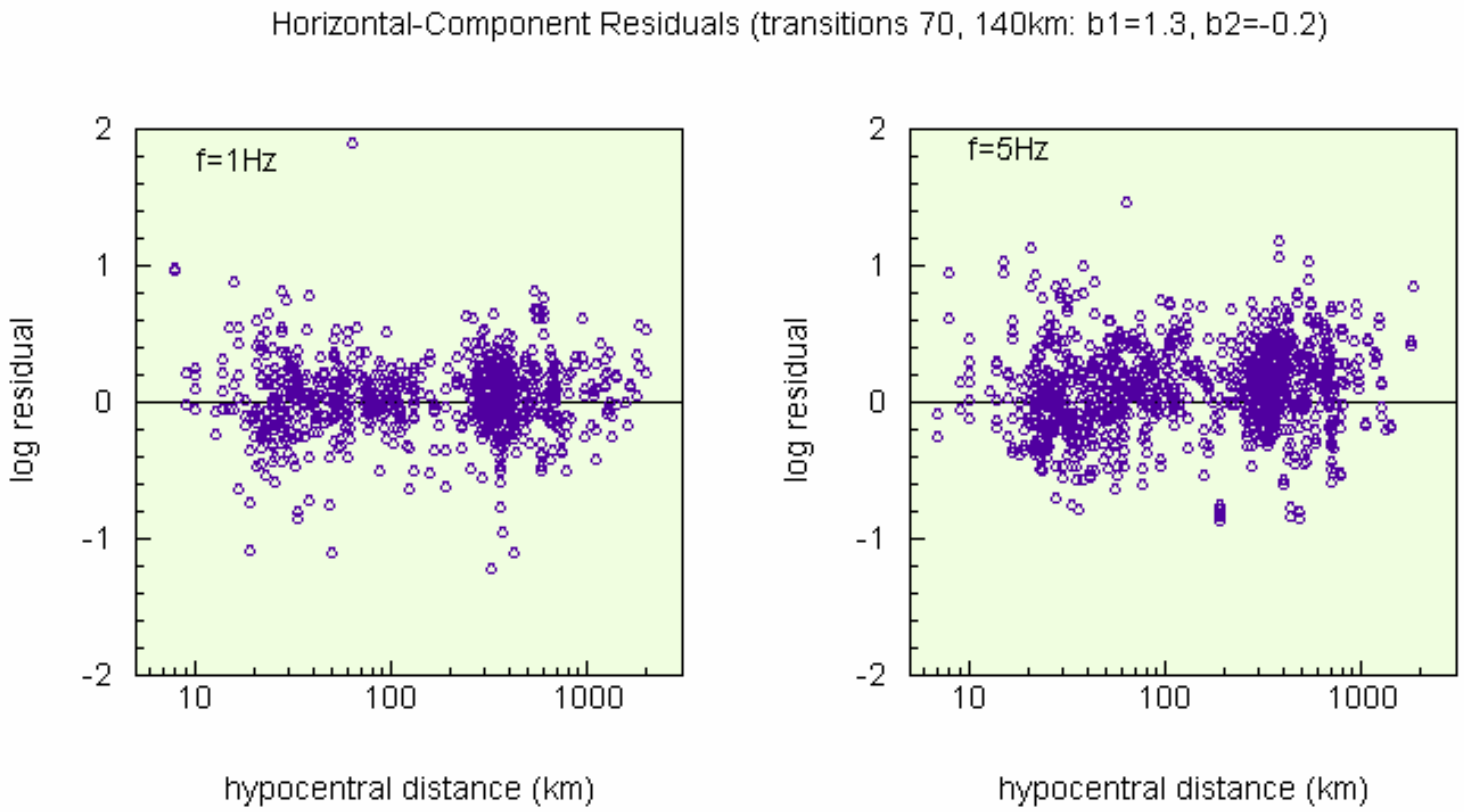

Mean H/V ratio for ENA rock sites:
increases with frequency from values near unity at 1 Hz to a factor of about 1.5 at high frequencies. This H/V is assumed to represent crustal to near-surface amplification effects for rock sites.

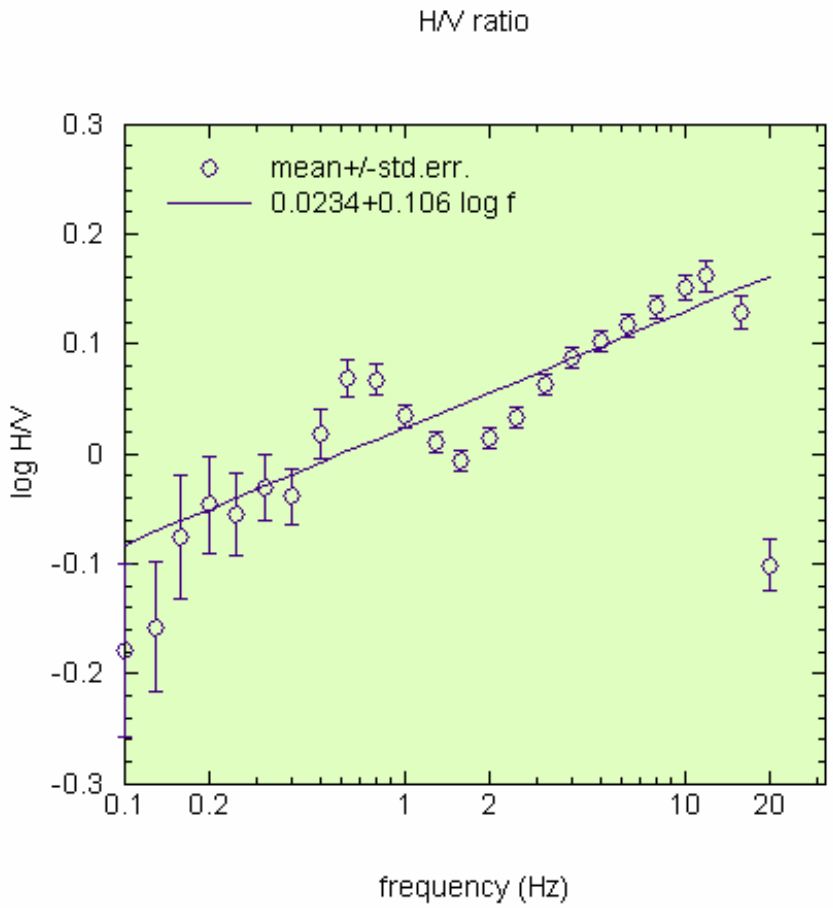

Attenuation results can be used to correct observations back to the source, to obtain apparent source spectra for individual earthquakes. Events of m1>4 follow Brune model with stress drop ~100 bars.

Thick black lines show Brune model spectra for 100 bars, for M=4, 5. Thin lines show source spectra for events of 4<m1<5

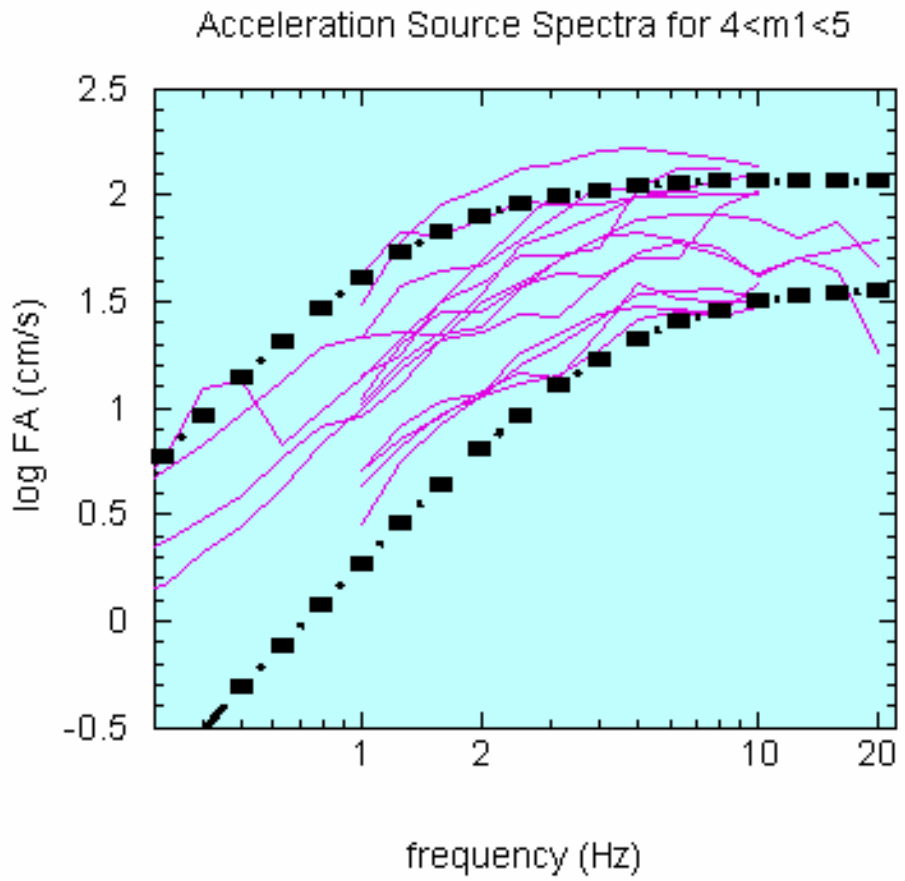

Data on high-frequency levels can be augmented by historical data based on felt areas.

Relationship between felt area and high-frequency spectral acceleration level (at a reference distance of 20 km). Symbols show data from Atkinson (1993a) (filled squares), data from Atkinson (2004) (open squares) and historical seismogram data of Atkinson and Chen (1997). Lines show least-squares fit.

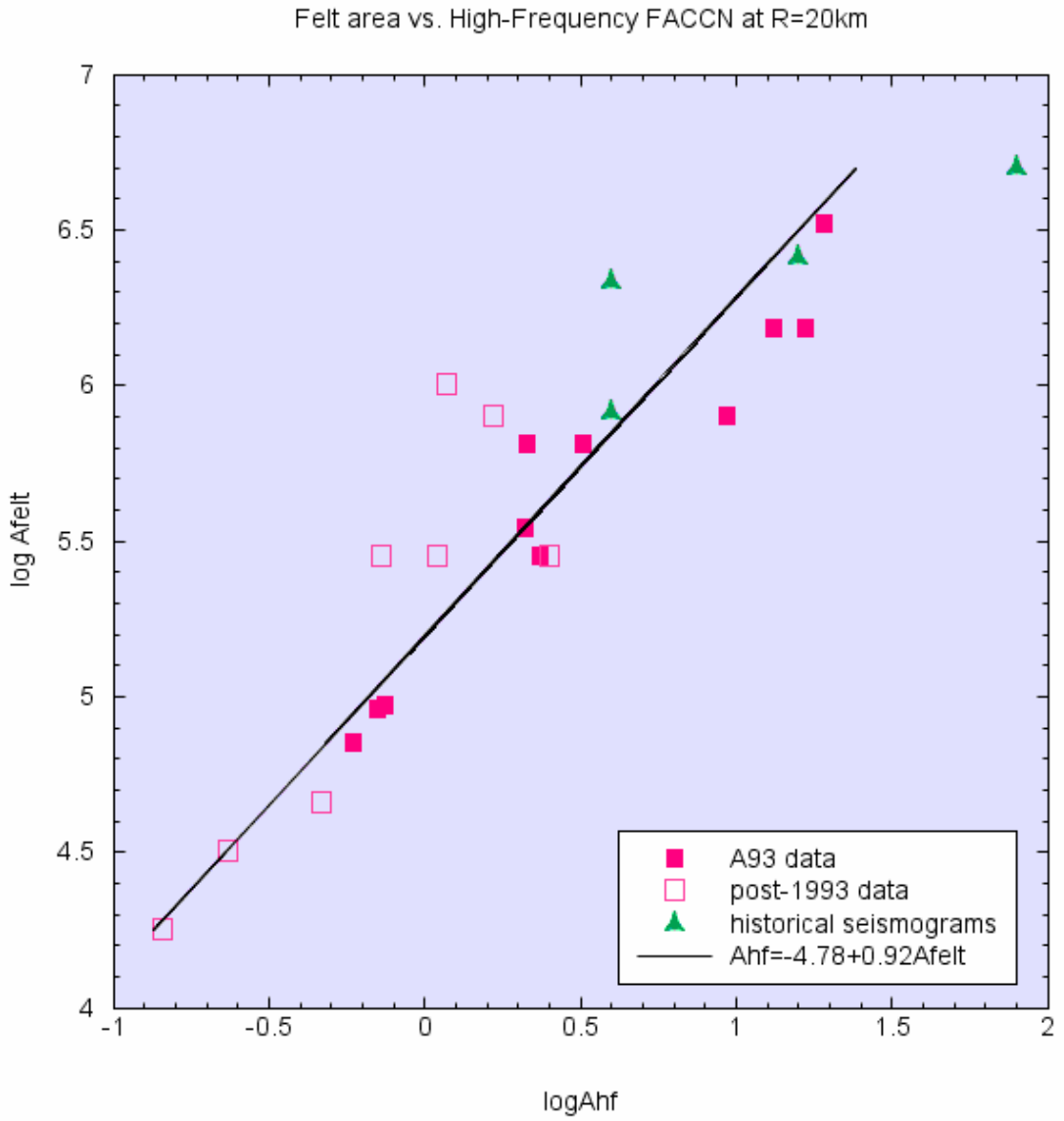

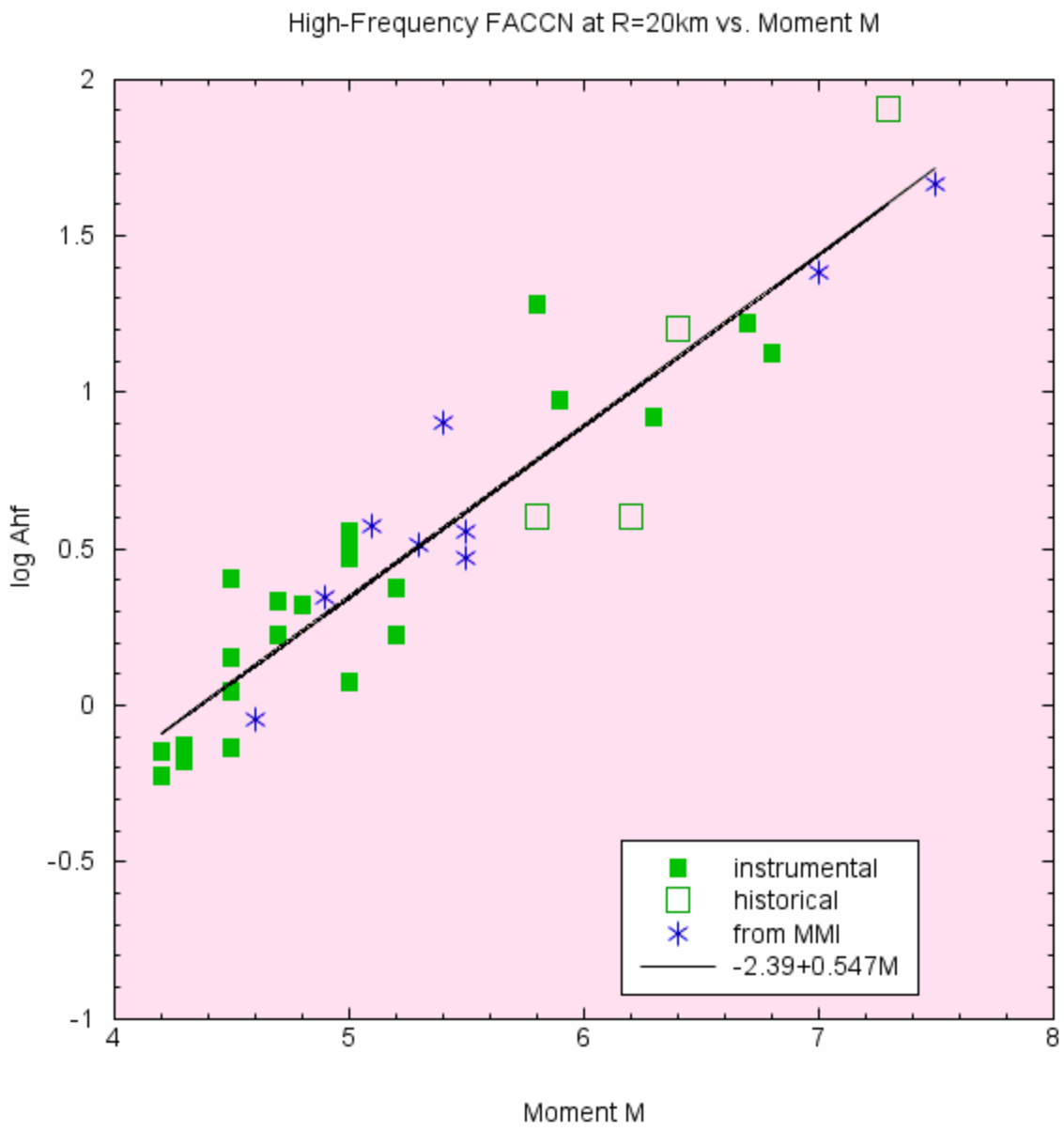

Compilation of ENA data on high-frequency levels, from both instrumental and historical data: this information can be used to infer stress drop

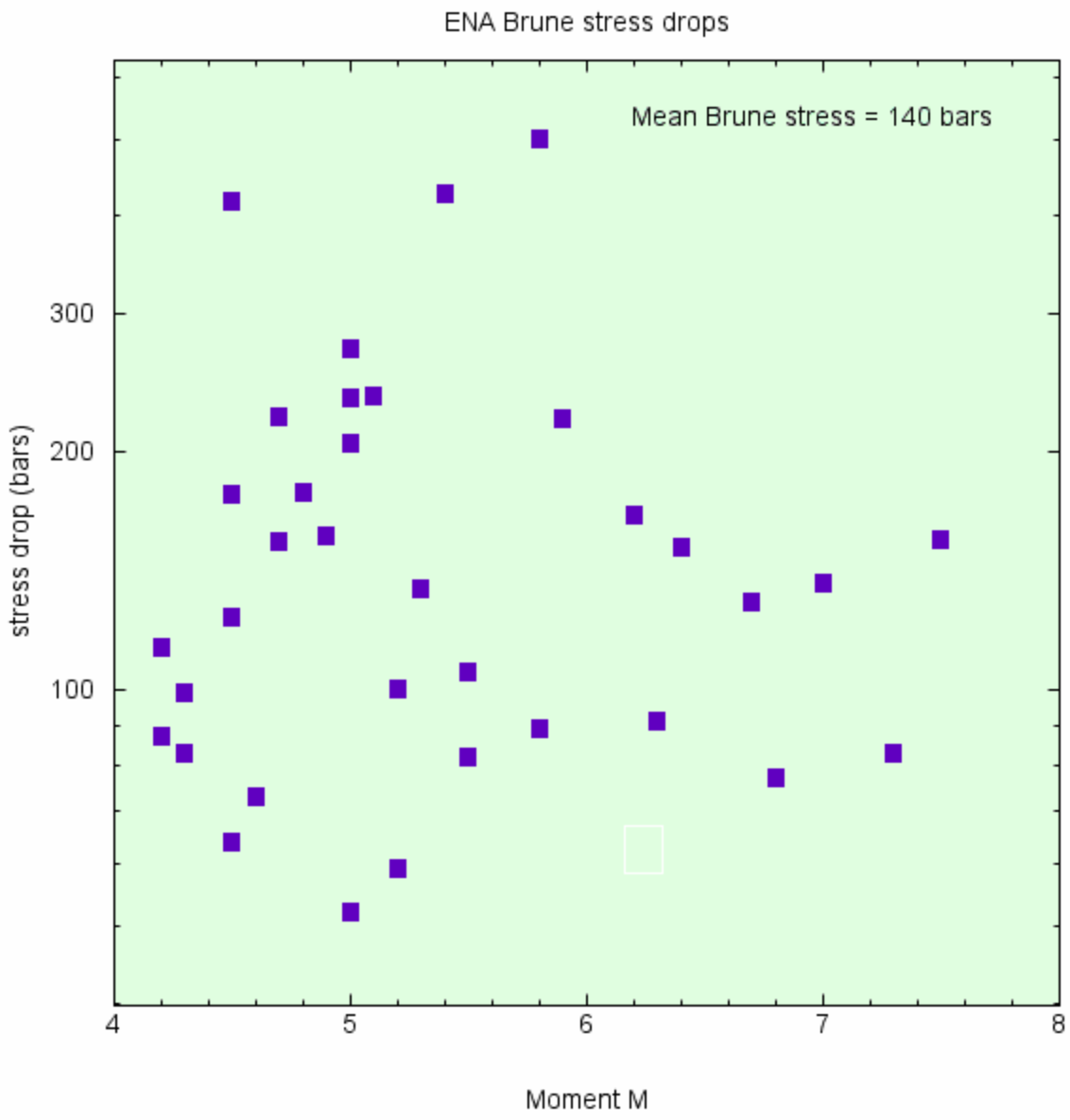

ENA stress drops, based on high-frequency spectral level. Mean = 140 bars.

AB05 simulations:
Log values of horiz, component 5% PSA at frequencies 0.5, 1, 5 Hz, and PGA, for ENA rock sites. Dots show PSA from simulations, including aleatory uncertainty, for M 5 (light) and M 8 (dark). Solid lines show predicted amplitudes from regression equations developed from simulated database, for M5, 6, 7, 8

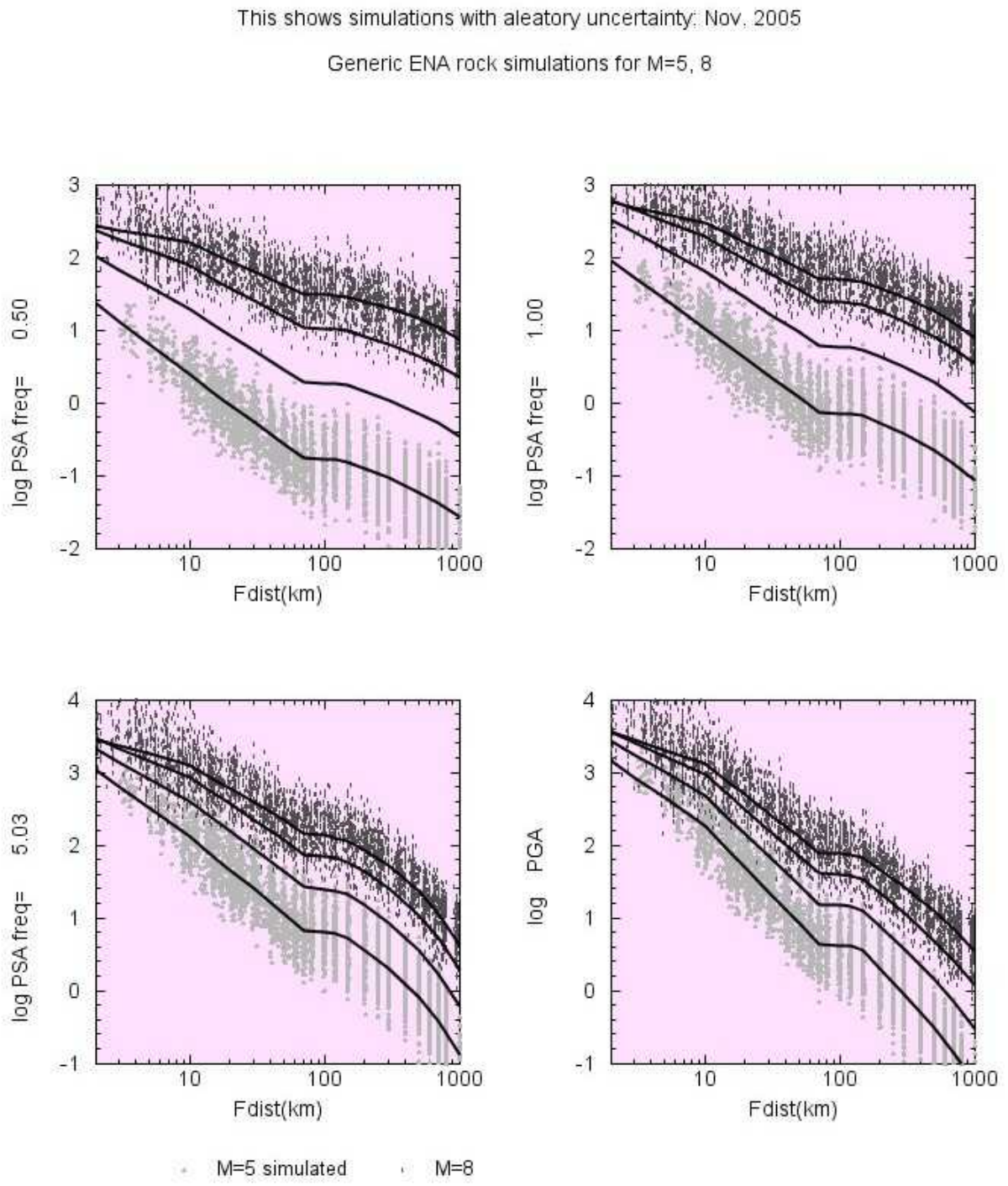

Example of regression residuals versus distance for M=6. Gray dots are individual residuals (where log residual = log simulated PSA – log PSA predicted by Equation 5). Black symbols show mean residuals and standard deviation in distance bins.

Sigma based on model is 0.3 log units for all frequencies (this is 0.69 ln units --- compare to WNA 2005 empirical value of 0.60 ln units)

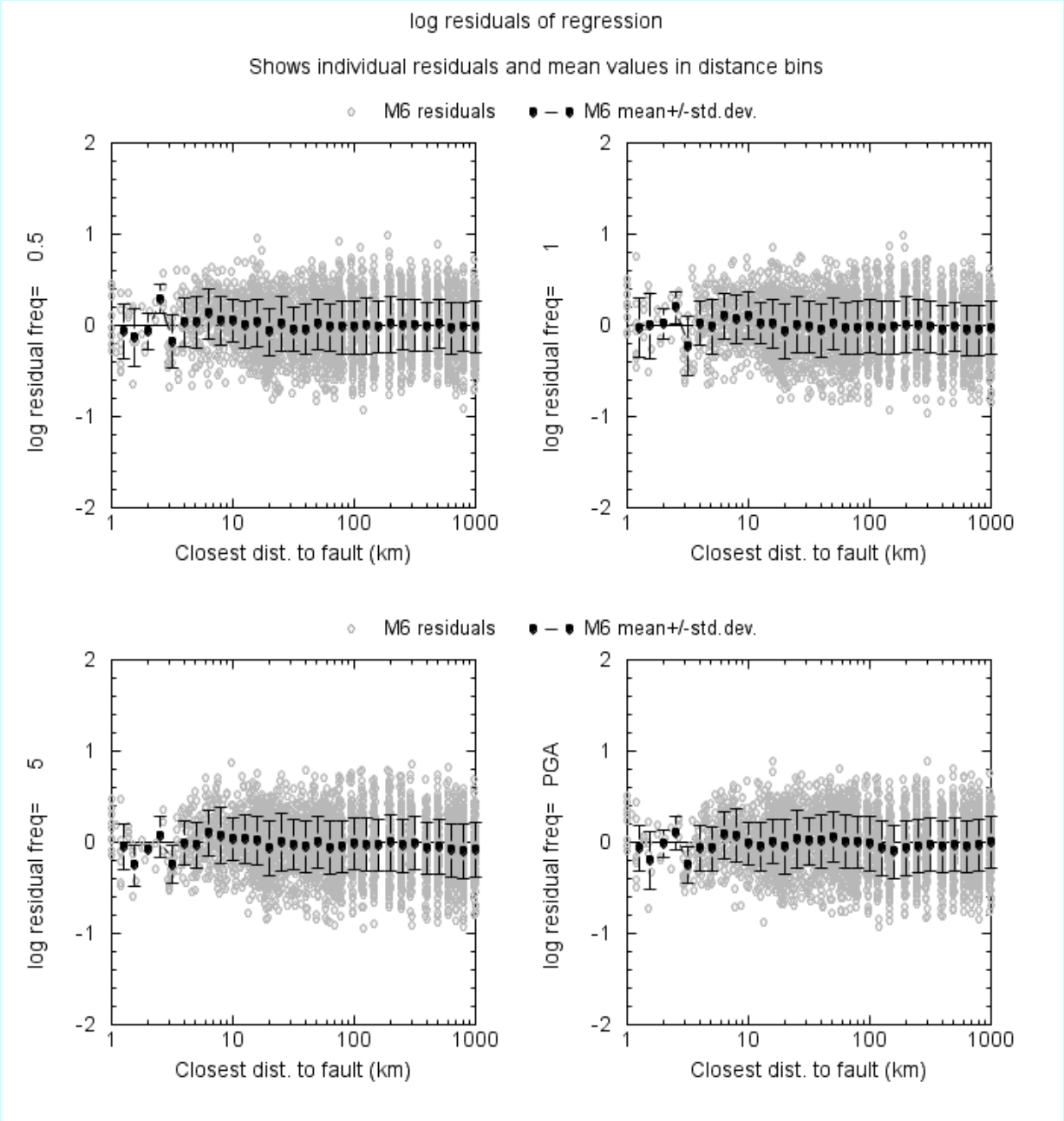

AB05 rock *simulations* (dark grey=mid-point M, light grey=+/- 0.5M);

equations **(black) ;**

data **(M-0.5 green, M+0.5 red)**

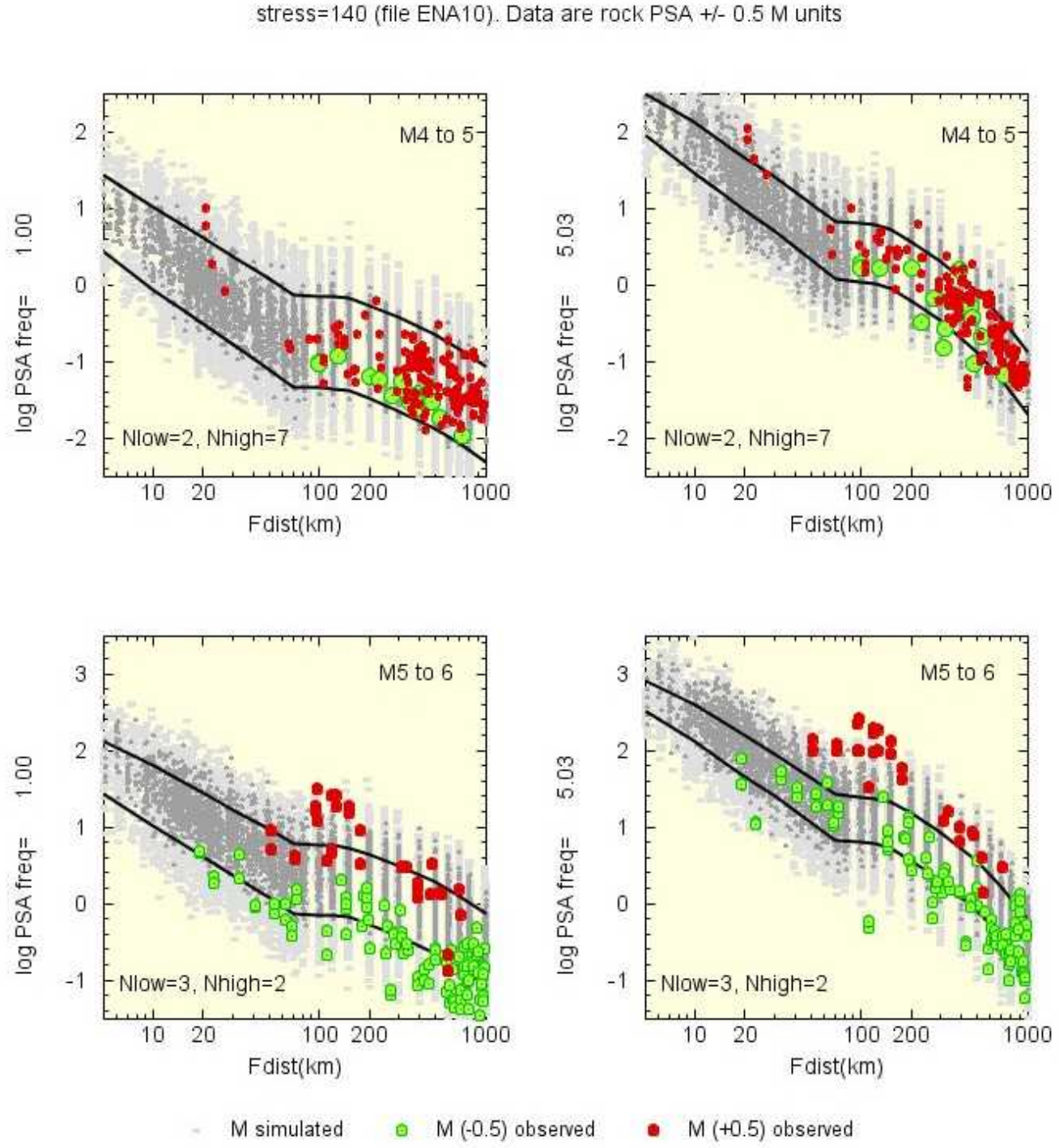

AB05 rock *simulations* (dark grey=mid-point M, light grey=+/- 0.5M);

equations **(black) ;**

data **(M-0.5 green, M+0.5 red)**

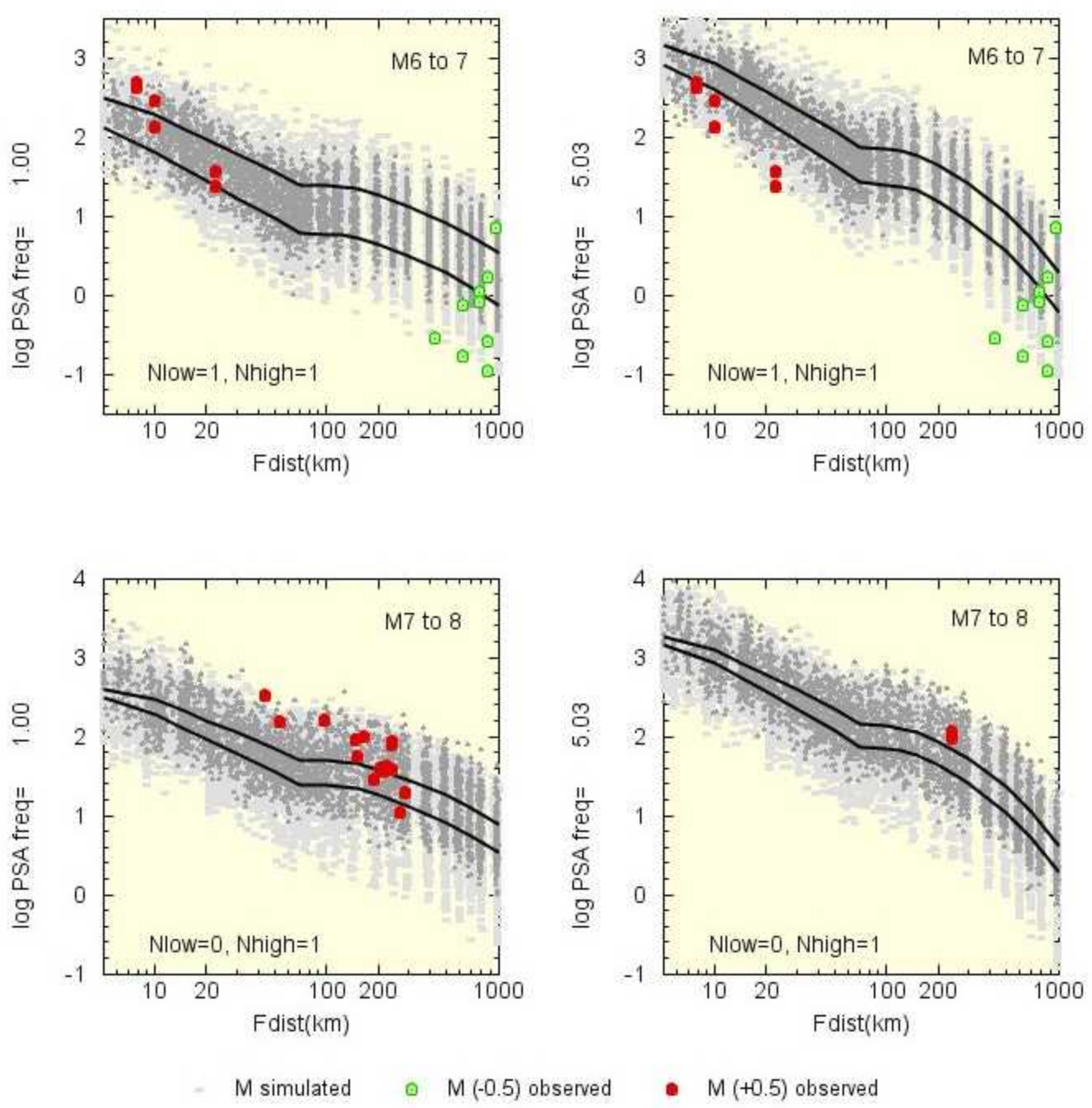

Residuals of ENA data relative to AB05

- Can compute residuals of ENA data relative to AB05 (=log obs. – log predicted)
- Keep in mind that these may not be = 0 as they represent only a subset of the information used in the model
- Overall average sigma within 0.06 log units of 0.0 over all frequencies from 0.5 to 5 Hz
- significant residuals are observed in some magnitude-distance ranges

Comparison of AB05 eqns to M4.9 2005 Riviere du Loup data

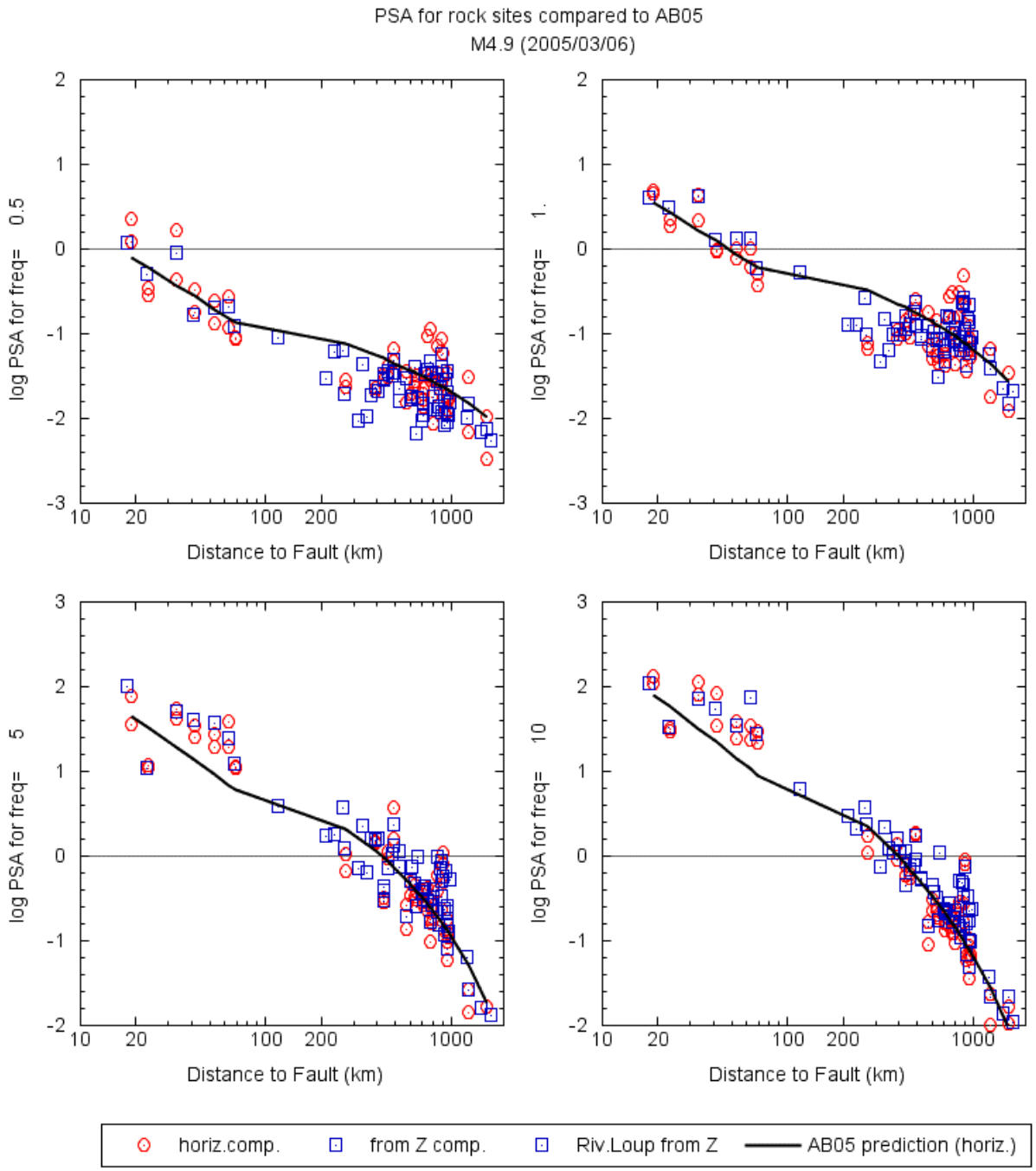

Comparison of AB05 eqns to several M4.5 events

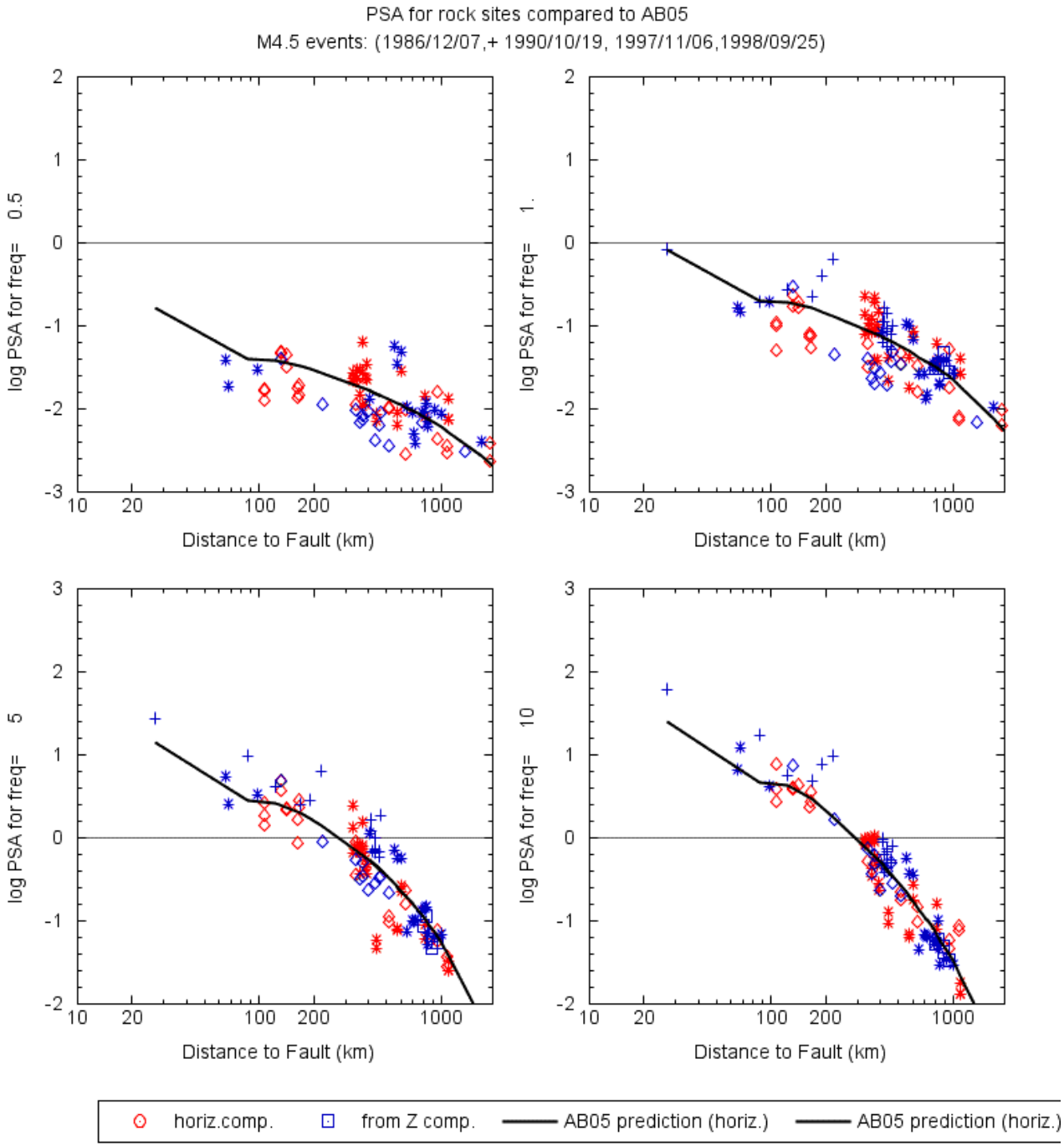

Comparison of ground-motion equations of this study (solid red lines) for M 5.5 and 7.5, with previous predictions (Atkinson and Boore, 1995, black), and mean and standard deviation of alternative EPRI (2004) predictions (blue), all for hard-rock site conditions in ENA.